Irrigation Science (2024) 42:1311–1332
https://doi.org/10.1007/s00271-024-00968-w

ORIGINAL PAPER

Estimating crop coefficients from canopy cover and height for a drip-irrigated young almond orchard: assessment using a two-source energy balance model

F. Montoya[1] · J. M. Sánchez[2] · J. González-Piqueras[2] · R. López-Urrea[3]

Received: 12 April 2024 / Accepted: 6 August 2024 / Published online: 2 September 2024

Abstract

The aim of this study was to estimate standard crop coefficients of surface and sub-surface drip-irrigated young almond trees under non-limiting soil water content conditions, based on measurements of the fraction of ground covered by the canopy (f_c) and tree height (h) (A&P approach proposed by Allen and Pereira (2009)) and to improve the transferability of them to the productive sector once weather data (i.e. maximum and minimum air temperature (T_{max} and T_{min}, respectively), as well as dew point temperature (T_{dew})) were adjusted to the reference conditions. A 4 year field experiment was carried out in a ~ 12.5 ha commercial young almond (*Prunus dulcis* (Mill.) D.A. Webb) orchard located in Hellín, (SE Spain). 'Penta' almond trees, grafted onto the GF-677 rootstock, were planted in 2018. Field measurements of f_c and h were performed over four consecutive growing seasons from 2019 to 2022. In parallel, ET_o computed by the nearest meteorological station, located at a non-reference weather site, was reduced around 6% after bringing weather data closer to the reference conditions, while actual crop evapotranspiration and its components (actual tree transpiration and soil evaporation) were estimated in each irrigation system through the so-called simplified two-source energy balance (STSEB) model in order to be used as a quality assessment of the A&P approach. The ratio between the former estimations and the ET_o allowed to compute STSEB-based crop coefficients. No significant differences in effective canopy cover ($f_{c\ eff}$) nor h were observed between the two irrigation systems, and thus the estimated K_{cb} values were the same for both drip-irrigation systems. $f_{c\ eff}$ values during mid-season stage ranged between 0.15 in 2019 and 0.62 in 2022, whereas average h values for this stage ranged between 2.36 and 3.80 m in 2019 and 2022, respectively. These values of $f_{c\ eff}$ and h resulted in average mid-season basal crop coefficients ($K_{cb\text{-}mid}$) of 0.28 in 2019, 0.39 in 2020, 0.61 in 2021 and 1.02 in 2022. Soil evaporation estimates through STSEB model were significantly different between the two irrigation systems, leading to differences in K_e being around 16% higher for DI than SDI. Moreover, the intra-annual K_c values moved in the same range for the initial, mid- and end-season crop growth stages, varying from 0.30 in 2019 to 1.01 in 2022, computed under standard conditions. Finally, the A&P approach was shown to be an especially interesting method for estimating K_{cb} values in almond fruit trees, being useful for refining K_{cb} and/or K_c for conditions of plant spacing, size and density that may differ from standard values. In this way, irrigation scheduling can be optimized regarding the almond tree architecture (i.e. $f_{c\ eff}$ and h), allowing to manage properly irrigation water to meet the tree water demands.

Introduction

In recent years, the global harvested area of almond trees has expanded significantly for various reasons, including the mechanization of harvesting, a considerable increase in global demand, which has led to a gradual increase in prices paid to the grower (Goldhamer and Fereres 2017); and the introduction of new late-flowering cultivars, which reduces the risk of production loss due to spring frost. Worldwide, more than 2.2 million ha of almond trees are cultivated, with Spain being the leading country by area, with more than

✉ F. Montoya
fms.itap@dipualba.es

[1] Instituto Técnico Agronómico Provincial de Albacete, Parque Empresarial Campollano, 2ª Avda. Nº61, 02007 Albacete, Spain

[2] University of Castilla-La Mancha, Regional Development Institute, Campus Universitario S/N, 02071 Albacete, Spain

[3] Desertification Research Centre (CIDE), CSIC-UV-GVA, Ctra CV 315, Km 10.7 Moncada, 46113 Valencia, Spain

744,000 ha, followed by the United States of America (USA) with around 534,000 ha. However, the USA is the world's foremost almond producer with a share of 55% of world production in 2021 (FAOSTAT 2022), whereas in Spain this share is 9% (MAPA 2023). This is because, although the irrigated area in Spain has almost tripled in the last 5 years, low-yielding traditional non-irrigated orchards still represent more than 80% of the cultivated area (MAPA 2023). This explains why Spain's average yields of shelled almonds are lower (0.49 t ha^{-1}) than those of the USA (4.10 t ha^{-1}) (FAOSTAT 2022), where the majority of almond orchards are fully-irrigated and managed under standard optimal conditions. In the Castilla-La Mancha region (i.e. the study area), the almond cultivated area has grown exponentially, reaching 150,453 ha in 2021, of which only 17% are irrigated. However, most of the new almond orchards are cultivated in traditional irrigated areas, replacing less profitable irrigated crops (Mirás-Avalos et al., 2023).

In arid and semi-arid areas with water resource scarcity, population growth and increasing water competition with other sectors, such as the industrial and urban sectors, improving almond water management is absolutely essential. In addition, in a global scenario of climate change, this situation appears to be worsening, mainly due to higher temperatures, less annual rainfall and an increasing number of extreme weather events (IPCC 2022). Under this context, in the study area, where water resources (mainly groundwater) are limited and at serious risk of overexploitation, it is impossible, in many cases, to apply irrigation regimes that cover the potential crop water requirements of almond trees. Therefore, measuring or estimating almond crop evapotranspiration (ET_c) and crop transpiration (T_c) under standard, well-watered conditions (i.e. under pristine, non-stress cropping conditions), and relate them to the FAO Penman–Monteith (FAO-PM) grass reference evapotranspiration (ET_o) equation (Allen et al. 1998), allow to derive single and basal crop coefficients (i.e. K_c and K_{cb}, respectively) as accurately as possible. However, when crop is managed under non-standard conditions due to non-uniform irrigation, water and/or salt stress, unsuitable soil management, etc. (Pereira et al. 2023; López-Urrea et al. 2024), the observations refer to actual crop ET ($ET_{c\ act}$) and not standard ET_c, with $ET_{c\ act} \leq ET_c$, being equal to ET_c only when the crop is well-watered and managed in a pristine condition (Pereira et al. 2023). The resulting actual K_c ($K_{c\ act}$) is calculated as the product of K_c by a stress coefficient (K_s), describing the effect of water and/or salt stress on crop ET. When using the dual crop coefficient method, only the K_{cb} is modified into $K_{cb\ act}$, as $K_{c\ act} = K_{cb}\ K_s + K_e$, thus affecting only crop transpiration, where the last term is the coefficient of soil evaporation not affected by stress (Allen et al. 1998). In this sense, obtaining crop coefficients values represent a key objective for optimizing the irrigation scheduling of this fruit tree, and identifying the best scheduling irrigation strategies when the almond water requirements cannot be met.

In the last decade, several studies have focused on the measurement of mature almond tree water requirements (Stevens et al. 2012; Goldhamer and Fereres 2017; López-López et al. 2018; Bellvert et al. 2018), being carried out in many cases with traditional cultivars ('Nonpareil' or 'Guara'). Similarly, young almond orchards have also been studied in recent years (García-Tejero et al. 2015; Espadafor et al. 2015; Drechsler et al. 2022), where the crop water requirements studies for new late and extra-late flowering cultivars are still quite scarce (Sánchez et al. 2021; Montoya et al. 2022). Different methods have been used to measure or estimate crop evapotranspiration in almond tree, such as the soil water balance (SWB) based on measuring the soil water content with neutron probe (López-López et al. 2018), weighing lysimeters (Espadafor et al. 2015), sap flow sensors or eddy covariance heat flux systems (Sánchez et al. 2021). Other methods of estimating crop water use are based on remote sensing surface energy balance models, either one- or two-source (Norman et al. 1995; Allen et al. 2007), which offer a higher spatial resolution than the SWB. In this research, a simplified version of the Two-Source Energy Balance (TSEB) model was used. In recent years, the TSEB, using field measurements of soil and canopy temperature, canopy height and fractional cover or leaf area index (LAI) as inputs, has proven to be a reliable approach for estimating almond ET_c and its separate components (soil evaporation (E_s) and canopy transpiration (T_c)) (Sánchez et al. 2021; Quintanilla-Albornoz et al. 2023).

Seasonal water use of young almond trees has been shown to vary greatly in accordance with tree density and orchard management practices, where the irrigation system method (i.e. micro-sprinkler vs. drip) can result in large differences in the crop evapotranspiration rates despite the fraction of ground covered by the canopy (f_c) being in the same ranges. Drechsler et al. (2022) reported seasonal actual crop evapotranspiration ($ET_{c\ act}$) of 888, 1075, and 995 mm for 3-, 4-, and 5-year-old micro-sprinkler irrigated almond trees, respectively, from full bloom until the end of harvest. In contrast, several studies carried out under drip irrigation system have reported lower accumulated $ET_{c\ act}$. Fereres et al. (1982) estimated between 114 and 643 mm of cumulative $ET_{c\ act}$ for 2 – 5 year-old almond trees in a field trial conducted in California, while the seasonal water use in a semiarid Spanish area was 321 mm, from March to October, in 3 year-old almond trees (Sánchez et al. 2021), and close to 600 mm and 450 mm of seasonal $ET_{c\ act}$ in a 4 year-old almond orchard managed under surface and sub-surface drip irrigation systems, respectively (Montoya et al. 2022).

Together with the measurement or estimation of the almond tree water requirements, studies have dealt with the derivation of single (K_c) and basal (K_{cb}) crop coefficients for

young and mature almond trees, representing the ratios of the ET_c and crop transpiration (T_c), respectively, to the grass reference evapotranspiration (ET_o), (i.e., $K_c = ET_c/ET_o$ and $K_{cb} = T_c/ET_o$; Allen et al. 1998; Pereira et al. 2024). These coefficients are an operative tool for farmers and technicians when irrigation scheduling is performed based on the daily crop water demand using the two step approach (Allen et al. 1998). It is worth noting those crop coefficients should be computed for an almond crop under pristine conditions (Pereira et al. 2015). In a recent review of K_c and K_{cb} for temperate climate fruit crops, included in this Special Issue, López-Urrea et al. (2024) identified a significant variability of those coefficients mainly due to differences in f_c and height (h) of almond tree, which are directly related to the training system, pruning and tree age. For mature trees, K_c values during the mid-season stage ranged between 0.33 and 1.23, while K_{cb} values ranged between 0.30 and 1.00 for the same stage (Stevens et al. 2012; López-López et al. 2018; Bellvert et al. 2018; Ramos et al. 2023). However, for young almond trees (less than 4 years), the reported mid-season K_c ($K_{c\ mid}$) and K_{cb} ($K_{cb\ mid}$) ranged between 0.30–0.90 and 0.19–0.50, respectively (Espadafor et al. 2015; Sánchez et al. 2021; Drechsler et al. 2022). Unlike the former stage, initial and end growth stages for both coefficients were less variables. During the initial stage, $K_{c\ ini}$ and $K_{cb\ ini}$ ranged between 0.40–0.50 and 0.15–0.30, respectively; and 0.20–0.55 ($K_{c\ end}$) and 0.18–0.50 ($K_{cb\ end}$) for end-season. This variability was also identified in mature almond trees by Rallo et al. (2021), although reporting K_{cb} values from literature between 0.45 and 1.00 during mid-season, and between 0.40 and 0.65 during end season, but not tabulating the coefficients related with canopy density on shading and on maximum relative ET (M_L), and the stomatal control of the tree on transpiration (F_r) (Allen and Pereira 2009).

As discussed above, K_c and K_{cb} values over the crop growing season are strongly related to a variety of vegetation parameters, including f_c, h, LAI or the fraction of the intercepted photosynthetic active radiation (f_{IPAR}) which is assumed as an estimate of f_c (Pereira et al. 2020b). Allen et al. (1998) introduced a standardized approach to relate K_{cb} during the midseason period, $K_{cb\ mid}$, to LAI or f_c using a K_{cb} value representing K_{cb} under conditions of full cover. Allen and Pereira (2009) later developed a method for predicting actual crops coefficients from f_c and h, (hereinafter the A&P approach), who showed that this approach performs particularly well for fruit trees and vines. Those actual crop coefficients are considered as standard when their estimates are based on fruit trees and vine crops managed under well-watered and pristine/eustress cropping conditions (Pereira et al. 2023; López-Urrea et al. 2024). Regarding fruit trees and vines, that approach, adopted in SIMDualKc model (Rosa et al. 2012a, b), has reported a good performance evaluating true ground ET_c measurements (i.e. Eddy Covariance and sap flow devices) for peaches (Paço et al. 2012), super-intensive olive orchard (Paço et al. 2014, 2019) and vineyards (Cancela et al. 2015); or with soil moisture sensors in citrus, pomegranate, olive and almond (Ramos et al. 2023). Recently, the A&P approach was validated and parameterized using ground and remote sensing data for several field and vegetable crops (Pereira et al. 2020b, 2021c). In the case of young and mature almond trees, Pereira et al. (2020b) did not report the validation of K_{cb} predicted from f_c and h using either ground or remote sensing observations although Ramos et al. (2023) obtained the 5 year-old almond' parameterization using SIMDualKc.

The standard FAO56 approach, for computing crop water requirements, uses ET_o calculated with the FAO-PM-ET_o equation) and a K_c (Allen et al. 1998; Pereira et al. 2024); where the latter represents an integration of the effect of four primary characteristics (i.e., crop height, albedo, canopy resistance and soil water evaporation) that distinguish a typical field crop from the grass reference in terms of the energy balance, and ET_o represents the actual evaporative demand of the atmosphere. According to the FAO56 method for computing ET_o, weather data must be measured above an extensive grass crop that is actively evapotranspirating, or in an environment with healthy vegetation not short of water. When these weather data are measured at a non-reference site (over non-transpiring, low-transpiring surfaces or having a short grass fetch), the reference rate of evapotranspiration cannot be attained because air temperatures measured at non-reference sites are higher than those that would have been measured if reference conditions had existed. The opposite occurs for the air relative humidity. One of the main issues of weather station networks around the world is related to their location, since most are not installed over an extensive grass surface or in an environment with healthy vegetation not short of water. In this sense, the present work seeks to improve the transferability of standard single and basal crop coefficients of young almond trees, adjusting the ET_o to the reference conditions.

This 4-year study was conducted with the aim of estimating standard crop coefficients for an extra-late flowering cultivar of young almond trees to improve estimates of almond trees-water requirements, using the FAO56 method (A&P approach), and a simplified two source energy balance model as a mean of quality control of data, in order to optimize the irrigation scheduling and make a more sustainable use of irrigation water during the early years of an almond orchard when its canopy architecture (i.e. f_c and h) is growing. To achieve this goal, it was proposed to: i) analyse the effects of using weather data obtained over non-reference sites on the calculation of ET_o; ii) estimate the K_{cb} values for drip-irrigated (surface and subsurface) young almond trees under standard, well-watered conditions, based on measurements of f_c and h (i.e., applying the A&P approach); iii)

assess the differences in the soil water evaporation (evaporation coefficient, K_e) and, hence, in the K_c values, between surface and subsurface drip irrigation systems; iv) assess and validate the crop coefficients predicted using of the A&P approach, harnessing $ET_{c\ act}$ estimates from a surface energy balance model (STSEB model).

Materials and methods

Study site description and orchard management

The present study was conducted over four consecutive cropping campaigns (2019–2022) within the framework of an irrigation trial carried out in a 0.9 ha area of a commercial almond orchard (Montoya et al. 2022). A brief description of the study site and orchard management is provided at follow, being the reader referred to Montoya et al. (2022) for further information.

The field experiment was conducted in a 12.5-ha commercial young almond orchard located in Albacete (SE Spain) (38° 29´ N, 1° 47´ W, 550 m a.s.l.). The climate is semiarid, temperate Mediterranean, with predominantly dry and warm summers. Long-term average annual rainfall is about 320 mm and the annual cumulative ET_o calculated with the FAO-PM-ET_o equation is about 1259 mm. The soil is classified as *Aridisol* with a fine-loam texture (USDA-NRCS 2014).

Almond trees (*Prunus dulcis* (Mill.) D.A. Webb) were planted in 2018 with cv. Penta grafted onto the GF-677 rootstock. Tree spacing was 5 m (within row) and 6 m (inter-row), resulting in 333 trees ha^{-1}. The average soil depth of the almond plot was 1.2 m, with there being a petrocalcic horizon underneath this soil depth. The ground surface of the almond orchard was maintained with bare soil. Soil tillage was carried out with a cultivator at different times per campaign, mainly after 5–7 days of a heavy rainfall, and the ploughing depth was 0.10 m during the experiment. The space between trees was maintained without weeds using herbicide in the two first crop-greening seasons.

Weather records during the 4-year experiment were measured with an agrometeorological station located at the experimental plot. The following variables were measured: air temperature and relative humidity, horizontal wind speed and direction, incoming-outgoing shortwave and longwave radiations, and rainfall. In addition, ET_o values were calculated daily by means of the FAO-PM ET_o equation (Allen et al. 1998), using the climate data provided by the "Ontur" meteorological station, the nearest ones to the experimental plot (~ 29 km.) belonging to the Spanish Agro-climatic Information System for Irrigation (SIAR 2022). In this field experiment, two drip-irrigation systems (surface, DI; and subsurface, SDI) were designed to meet the full crop water requirements. Each treatment was arranged with 4 replicates in a complete block randomized design.

Correction of weather data affected by aridity conditions to compute reference evapotranspiration

The "Ontur" meteorological station (latitude 38º 37' north, longitude 1º 29' west and 695 m above sea level; SIAR 2022), as most of the Spanish network of weather stations and others around the world, is located in a cropped area where the recorded meteorological data are measured in atmospheric conditions similar to those for the surrounding crops. However, a criterion for establishment, i.e. being sited on an extensive surface of irrigated grass or short crop, is typically not met.

Allen et al. (1998) reported that ET_o computed from standard estimates for available energy (net radiation, R_n, minus soil heat flux, G), aerodynamic resistance (r_a) and surface resistance (r_s), would overestimate those calculations using meteorological data of air temperature and vapour pressure deficit under non-reference conditions ($T_{n/ref}$ and $VPD_{n/ref}$, respectively). This is because $T_{n/ref}$ are higher than those measured if reference conditions had existed, and relative humidity measured at a non-reference site is lower than that which would have occurred under reference conditions ($VPD_{n/ref} > VPD_{ref}$). Therefore, a correction is required to bring temperature and humidity data closer to the reference conditions. This is the case of the "Ontur" weather station, the observed meteorological data from which were recorded at a non-reference site.

Following the correction process proposed by Allen et al. (1998) and Pereira et al. (2024), maximum and minimum air temperature (T_{max} and T_{min}, respectively), as well as dew point temperature (T_{dew}), were corrected in proportion to the difference (T_{min}—T_{dew}), comparing the (T_{min}—T_{dew}) from the non/reference set to (T_{min}—T_{dew}) from the reference site. The reference weather station used for the corrections was located at "Las Tiesas" experimental farm (latitude 39º 14' north, longitude 2º 5' west and 695 m above sea level). At this site, there is a 1.5-ha standardized vegetated (grass) surface (*Festuca arundinacea* Schreb., cv. ''Asterix'') of uniform height, actively growing and not short of water, with the aim of measuring ET_o using a large weighing lysimeter. In addition, a weather station is available to record the meteorological variables necessary to calculate ET_o with the FAO-PM equation (López-Urrea et al. 2006; Trigo et al. 2018). To the best of our knowledge, this is the nearest site to the "Ontur" weather station (69.8 km far away) meeting all reference conditions.

In this sense, the following process was implemented to adjust T_{max}, T_{min} and T_{dew}, and then to compute the final, already corrected, ET_o values (Allen et al. 1998).

1. By a graphical procedure, compare T_{min}—T_{dew}, either daily or monthly data, from a non-reference site with those from a reference site using monthly ratios of precipitation/ET_o as the abscissa. Monthly data were considered for this study.

2. When monthly (or daily) differences T_{min}—T_{dew} for the non-reference site are systematically higher than the reference site, compute the average differences (ΔT) for those time steps which require correction.

$$\Delta T = \left(T_{min} - T_{dew}\right)_{n/ref} - \left(T_{min} - T_{dew}\right)_{ref} \quad (1)$$

3. Adjust temperatures for each type of time step used (daily or monthly).

$$\left(T_{max}\right)_{cor} = \left(T_{max}\right)_{obs} - (\Delta T/2) \quad (2)$$

$$\left(T_{min}\right)_{cor} = \left(T_{min}\right)_{obs} - (\Delta T/2) \quad (3)$$

$$\left(T_{dew}\right)_{cor} = \left(T_{dew}\right)_{obs} + (\Delta T/2) \quad (4)$$

4. Compute a new ET_o with the corrected values for T_{max}, T_{min} and T_{dew}. This correction was carried out for the 4-year study using this same temporal horizon (2019–2022) for both sites (i.e. Las Tiesas reference conditions vs. Ontur non-reference conditions).

Irrigation management, soil, and trees determinations

Irrigation was managed in the almond orchard to maintain non-limiting soil water content. For this purpose, a daily irrigation schedule was implemented, based on the SWB following the FAO56 approach (Allen et al. 1998; Pereira et al. 2020a). Crop evapotranspiration (ET_c) was computed by multiplying the grass reference evapotranspiration (ET_o) by a dual crop coefficient, consisting of a basal crop coefficient (K_{cb}) and an evaporation coefficient (K_e) representing the crop transpiration (T_c) and soil evaporation (E_s), respectively ($K_c = K_{cb} + K_e$) (Allen et al. 1998, 2005). The K_{cb} values used were: $K_{cb\ ini}$ (initial stage): 0.15; $K_{cb\ mid}$ (mid-season): 0.85; and $K_{cb\ end}$ (end-season): 0.35, which represents K_{cb} prior to leaf drop. $K_{cb\ mid}$ was adjusted to local climate conditions when different to standard conditions (i.e. minimum relative humidity (RH_{min}) of 45% and wind speed (u_2) of 2 m s^{-1}). Additionally, K_{cb} was reduced using the shading factor (K_r) reported by Fereres et al. (2012).

The first two extensions proposed by Allen et al. (2005) were adopted to calculate the total evaporation and drying process. In this sense, the soil evaporation coefficient calculation was divided into two separate terms ($K_{e\ SWB} = K_{ei} + K_{ep}$; Allen et al. 2005); the first was done for the exposed fraction of the soil wetted by both precipitation and irrigation (f_{ewi}), and the second was only for the fraction of the soil wetted by precipitation (f_{ewp}). The average fractions of soil wetted by DI and SDI were 0.12 (considering a wetting bulb for every drip line with a width of 0.40 m) and 0.01, respectively, while the fraction of the soil surface wetted by precipitation was 1.00. The readily evaporable water (REW) and the total evaporable water (TEW) were 8.0 and 18.1 mm, respectively. Finally, the transpiration rate from the surface layer of 0.10 m was also considered in the SWB (Allen et al. 2005).

The almond trees phenological stages were determined following the scale designed by Thomas (2018). Observations were carried out every 10–15 days starting by February until mid-December in each season (Table 1). The four main growing stages associated with the FAO segmented crop coefficient curve (Allen et al. 1998) were merged to the main almond phenological stages, defining the initial stage from swollen bud to onset of fruit set, crop development from onset of fruit set to fruit final size, mid-season from fruit final size to fruit ripening and end-season from harvest to onset of leaf fall (full tree maturity). The former stage is typically represented for tree conditions when both vegetative and reproductive buds have already differentiated. This growth stage, in terms of $f_{c\ eff}/f_c$, is usually represented by around 0.10 less of the maximum ground cover reached by the tree (Pereira et al. 2023).

The length of each phenological stage was estimated based on thermal time (Mcmaster and Wilhelm 1997), with 4.5 ºC as the base temperature (T_{base}) and 35 ºC as the upper temperature (T_{upper}) (Paredes et al. 2024a), the values of which were represented as cumulative thermal time or growing degree days (CGDD). Daily GDD was computed based on the difference of the average air temperature (T_{avg}; ºC) and T_{base}. Meanwhile, T_{avg} was calculated as the average of the maximum and minimum air temperature (T_{max} and T_{min}, respectively). Daily GDD was adjusted following the same rules proposed by Raes et al. (2023), described as follows:

$$T_{avg} = \frac{\left(T_{max} +\right)}{2} \quad (5)$$

- If T_{avg} is less than T_{base}, then $T_{avg} = T_{base}$
- If T_{avg} is greater than T_{upper}, then $T_{avg} = T_{upper}$

Determinations of the f_c were performed on 9 times on 16 trees in the three first cropping campaigns and 7 times in the last growing season. During the first and the last growing season of this study, digital photographs were taken at solar noon, vertically from an approximate height of 3.0 m above the tree canopy (eight plants per treatment). The CANOPEO software (Patrignani and Ochsner 2015) was used to obtain

Table 1 Duration in days and cumulated growing degree days (CGDD) of the four main growing stages associated with the FAO segmented crop coefficient curve (Allen et al. 1998) for almond trees across the study seasons (2019–2022)

Season	Duration	The FAO56 four crop growth stages			
		Initial	Crop development	Mid-season	Late-season
2019	Date	19-Feb to 26-Mar	27-March to 7-May	8-May to 1-Sep	2-Sep to 31-Oct
	DA-Swb	35	77	194	254
	CGDD	250	600	2,765	3,644
2020	Date	30-Jan to 20-Mar	21-Mar to 30-Apr	1-May to 28-Aug	29-Aug to14-Oct
	DA-Swb	50	91	211	258
	CGDD	365	654	2,819	3,512
2021	Date	2-Feb to 30-Mar	31-Mar to 29-Apr	30-Apr to 27-Aug	28-Aug to 10-Oct
	DA-Swb	56	86	206	250
	CGDD	349	607	2,694	3,436
2022	Date	4-Feb to 3-Apr	4-Apr to 25-Apr	26-Apr to 27-Aug	28-Aug to 9-Oct
	DA-Swb	58	80	204	247
	CGDD	348	532	2,765	3,124
2019–2022	CGDD (avg)	328	598	2,761	3,522
	CGDD (sd)	53	69	60	81
	CGDD (CV)	16.1	25.6	2.8	10.7

Date: first and last day of each growth stage; DA-Swb: days after swollen bud; CGDD cumulated growing degree days (ºC) from swollen bud, avg average, sd standard deviation, CV coefficient of variation (%), Initial period from swollen bud to onset of fruit set, Crop development period from onset of fruit set to fruit final size, Mid-season period from fruit final size to ripening fruit, Late season from fruit ripening to onset of leaf drop

the f_c value of each image using a white reference of known surface area. However, f_c was estimated in the second and the third campaign by measuring close to midday the fraction of intercepted photosynthetic active radiation in one central tree in each experimental plot. A SunScan™ canopy analysis system (Delta-T Devices Ltd., Cambridge, UK) was used to take measurements of photosynthetic active radiation data above and below the tree canopy over a fixed mesh of 66 reading points covering the planting frame of a tree. For further information, reader is referred to Montoya et al. (2022). In parallel to the f_c monitoring, tree height (h) was also measured on the same 16 trees across the four growing seasons. Using a measuring tape, h was measured between 10 and 13 times during the first three campaigns, while it was sampled three times in the last season.

In this study, the soil and plant water status were tested, respectively, by volumetric soil water content (VSWC) and midday stem water potential (SWP) measurements. VSWC was continuously monitored at 15-, 30-, 45- and 60-cm depths, using a set of four FDR sensors (model 10HS, Decagon Devices, WA, USA) installed at four different points on the plot (two monitor points per irrigation system) and close to the drip line (around 0.10 cm away to the drip line and distanced 1.0 m to the main stem of the tree). All hourly data were stored in four dataloggers (EM50, Decagon Devices, WA, USA). The reader is referred to Montoya et al. (2022) for further information. Determinations of SWP were conducted with a pressure chamber (model 600, PMS Instrument Company, Albany, OR, USA) on a leaf from each of 16 trees (8 trees monitored per treatment). This pressure chamber was calibrated before the start of the first and the third growing seasons. The measurements were performed close to solar noon on mature leaves located in the lower third of the canopy that were covered with a foil-laminate bag for at least one hour before being excised from the tree (Fulton et al. 2014). The total number of measurement days was 10, 12, 9 and 4 in 2019, 2020, 2021 and 2022, respectively. The behaviour of f_c, h and SWP in this almond orchard for the 2019–2021 field experiments was already described and analysed by Montoya et al. (2022).

*Brief description of the A&P approach (*Allen and Pereira 2009*) and K_c/K_{cb} computation*

The procedure for estimating the crop coefficients based on measurements of f_c and h, firstly initiated by Allen et al. (1998) and later detailed in Allen and Pereira (2009) (A&P approach), can be quite accurately estimated through their relationships with f_c, h and the amount of the stomatal regulation under soil moist conditions (Pereira et al. 2020b). According to Allen and Pereira (2009) a standardized method to relate the basal K_c during the mid-season period, $K_{cb\ mid}$, to f_c is by using K_{cb} values representing K_{cb} under conditions of full cover, $K_{cb\ full}$, which is represented by LAI > 3 (Pereira et al. 2020b). The K_c values are reduced when plant density or leaf area fall below full ground cover. In the same way, K_{cb}, which represents mostly transpiration, can be expressed in terms of a density coefficient (K_d) that

is estimated as a function of effective f_c ($f_{c\,eff}$). We estimated $f_{c\,eff}$ using the f_c measured (Fig. 3a-d) and the mean angle of the sun above the horizon during the period of maximum evapotranspiration, as described by Allen and Pereira (2009) and Oyarzun et al. (2007).

$$K_{cb} = K_{c\,min} + \left(K_{cb\,full} - K_{c\,min}\right) \quad (6)$$

where $K_{c\,min}$ is the minimum basal K_c for bare soil ($K_{cb\,min} \sim 0.15$ under typical agricultural conditions), $K_{cb\,full}$ is the estimated basal K_c during peak plant growth for conditions having nearly full ground cover (or LAI > 3).

$$K_d = min\left(1, M_L \times f_{ceff}, f_{ceff}^{(1/(1+h))}\right) \quad (7)$$

where $f_{c\,eff}$ is the effective fraction of ground covered by vegetation [0.01–1] near solar noon, M_L is a multiplier on $f_{c\,eff}$ describing the effect of canopy density on shading and on maximum relative ET per fraction of ground shaded [1.0–2.0], and h is the mean height of the trees in meters.

A resistance correction factor (F_r) was proposed for the LAI- and f_c-based equations to take stomatal control by vegetation into consideration (Pereira et al. 2020b). Thus, $K_{cb\,full}$, when used with ET_o, can be adjusted as a function of plant height, the climate and the stomatal control on transpiration (F_r, [0–1]). For further information about the description of the A&P approach, the reader is referred to Allen and Pereira (2009) and Pereira et al. (2020b).

$$F_r \approx \frac{\Delta + \gamma \times \left(1 + 0.34 \times u_2\right)}{\Delta + \gamma \times \left(1 + 0.34 \times u_2 \times \frac{r_l}{100}\right)} \quad (8)$$

where r_l is the mean leaf resistance for the vegetation (s m^{-1}), Δ is the slope of the saturation vapour pressure vs. air temperature curve (kPa $°C^{-1}$), and γ is the psychrometric constant (kPa $°C^{-1}$), both relative to the period when $K_{cb\,full}$ is computed.

$$K_{cbfull} = F_r \times \left(min(1 + 0.1 \times h, 1.20) + \left[0.04 \times (u_2 - 2) - 0.004 \times (RH_{min} - 45)\right] \times \left(\frac{h}{3}\right)^{0.3}\right) \quad (9)$$

where h is the mean maximum plant height in m, u_2 is the mean value for wind speed at 2 m height during the mid- and/or end-season in m s^{-1}, and RH_{min} is the mean value for minimum daily relative humidity during the mid- and/or end-season in %.

Following the former procedure, as well as considering the new M_L and F_r values tabulated for almond trees by López-Urrea et al. (2024), daily almond K_{cb} values were computed using the f_c and h measurements sampled along each growing season. After predicting K_{cb} values applying the A&P approach ($K_{cb\,A\&P}$), K_c values for each stage (i.e., initial, mid- and end-season) were estimated adding K_e values calculated using the method proposed by Allen et al. (2005) ($K_{e\,SWB}$) to $K_{cb\,A\&P}$. The obtained mid- and end-season K_{cb} and K_c values upper than 0.45 were adjusted to a standard temperate climate (i.e., sub-humid climate with moderate wind speed), characterized by minimum relative humidity (RH_{min}) of 45% and wind speed (u_2) of 2 m s^{-1}, using the equation reported by Allen et al. (1998). However, when these K_c and K_{cb} values were lower than 0.45, this adjustment was not required (Pereira et al. 2021b).

Brief description of the STSEB model

Based on the parallel approach introduced by Norman et al. (1995), a simplified version of the Two-Source Energy Balance (STSEB) model was initially proposed by Sánchez et al. (2008). The basis of the STSEB modelling for crop evapotranspiration (ET_c), including its soil evaporation (E_s) and canopy transpiration (T_c) components, stands on the conversion of the total latent heat flux (LE) and its soil and canopy components (LE_s and LE_c, respectively), by dividing them by the latent heat of vaporization of water, denoted as λ (J kg^{-1}). This turbulent energy flux can be approximated as a residual from the surface energy balance equation once net radiation (R_n) and soil (G) and sensible heat (H) fluxes are computed. For a comprehensive understanding of the mathematical framework and necessary inputs and parameters, readers are referred to Sánchez et al. (2021) where a proper calibration and evaluation of this model was carried out using eddy covariance system data as a reference, and adopting the quality control criteria of the ET estimates given by Allen et al. (2011a, b).

In this study, ground observations of tree canopy height and fractional green vegetation cover (outlined above) were utilized to model these inputs within the STSEB framework, employing a third-order polynomial adjustment. Two sets of 3–4 thermal InfraRed Thermometers (IRT) each (SI-121 and SI-421, Apogee Instruments, Inc., Logan, USA) were installed on two masts to continuously monitor the radiometric temperature of both the almond tree canopy and soil at separated locations representing both DI and SDI irrigation treatments. Three of the IRTs were positioned downwards at a 45° angle, two directed towards the canopy top on the east and west sides of trees, and the third pointing to the inter-row soil. The mast in the DI treatment area was equipped with an additional IRT monitoring the exposed fraction of soil wetted by surface drip irrigation in order to accurately characterize soil temperature in this scenario. This comprehensive set of thermal measurements included an extra IRT pointing upwards to measure downwelling sky radiance, which is essential for atmospheric correction of all soil and canopy temperatures. The experimental setup, including location and installation height, was designed to

ensure representative monitoring of each target, accounting for the field of view of the IRTs. Continuous 15-min IRT readings were collected to properly capture the surface energy fluxes. All measurements underwent corrections for atmospheric and emissivity effects following the methodology detailed in Sánchez et al. (2008).

Daily ET_c values and the T_c/E_s partition, derived from the STSEB model along with available thermal infrared data, were obtained for 251 days in 2019 (April 4 to December 12), only 152 days in 2020 (June 5 to November 3) due to pandemic-related constraints, then 286 days in 2021 (February 18 to November 30), and finally 223 days (March 2 to October 10) in 2022 (this year excluding a few weeks in mid-season for DI treatment due to an experimental failure with one of the IRTs). Daily almond K_c, K_{cb}, and K_e values were computed as the ratios ET_c/ET_o, T_c/ET_o, and E_s/ET_o values, respectively. The ET_o values computed after weather data correction, presented below, were also used for the STSEB estimates. To avoid the scatter produced by irrigation events, crop coefficient values were averaged in a 5-day time step.

Statistical analysis and evaluation of A&P approach performance

Calculated values of ET_o (corrected and non-corrected) from the "Ontur" meteorological station were compared using linear regression analysis (the intercept, slope, coefficient of determination (R^2) and significance of the linear model) to determine the consistency of said regression. The significance levels used were: $p \geq 0.05$ not significant; $0.01 \leq p < 0.05$ significant; and $p < 0.01$ very significant.

To evaluate the A&P approach estimating K_{cb} and K_c, we used a previous statistical analysis for almond K_{cb} and K_e, through an intra-annual analysis of variance (ANOVA; mean comparison test) and normality and homoscedasticity tests (Shapiro–Wilk and Barlett test, respectively), in order to determine whether the K_{cb} estimations obtained by the A&P approach and STSEB model were different between the two irrigation systems described in this work (i.e. DI and SDI). The same procedure was carried out for K_e calculated and estimated through the SWB and STSEB model, respectively. In the cases where the null hypothesis of the normality test was false, a non-parametric test (Mann Whitney: Wilcox test; median comparison test) was used instead of ANOVA. When the ANOVA or Mann Whitney test showed no evidence of the null hypothesis, the average value of K_{cb} and/or K_e of both treatments was proposed to study the A&P approach performance.

Subsequently, the K_{cb} values obtained by the A&P approach ($K_{cb\ A\&P}$) and STSEB model ($K_{cb\ STSEB}$) were compared for every growing season, as well as for all the years together, to evaluate the performance of the A&P approach. In this evaluation, $K_{cb\ A\&P}$ and $K_{cb\ STSEB}$ were considered as estimated values, representing graphically $K_{cb\ A\&P}$ in the ordinate axis and $K_{cb\ STSEB}$ in abscissa axis. In the same way, K_e, calculated by the SWB approach ($K_{e\ SWC}$) (Allen et al. 2005), and K_c, as the addition of $K_{e\ SWC}$ and $K_{cb\ A\&P}$, were compared to the values reported by the STSEB model (i.e. $K_{e\ EB}$ and $K_{c\ STSEB}$). These evaluations were carried out using the following statistical indicators: the root mean square error (RMSE), the mean bias error (MBE) and the index of agreement (d) (Willmott 1982). Linear regressions coefficients were performed through the Deming method since both approaches used to estimate K_{cb} are subjected to errors, despite STSEB method has been considered as the reference approach in this research (Linnet 1990). Finally, the average K_c and K_{cb} values obtained for each stage by the A&P approach were standardized and compared with the new updated K_c/K_{cb} values reported by López-Urrea et al. (2024). R Core Team (2021) was used to perform the statistical analysis.

Results

Meteorological conditions and ET_o values computed after weather data correction

The daily meteorological conditions during the 2019–2022 almond growing seasons at the experimental site for average air temperature and relative humidity (Fig. 1a), solar radiation and average wind speed (Fig. 1b) and ET_o (Fig. 1c) were typical of the long-term average weather conditions in the southeast of Spain. Compared to the 20-year mean in the area, rainfall was especially above average during the three first seasons, being about 28%, 68% and 32% higher in 2019, 2020 and 2021, respectively, while total precipitation in 2022 was similar to the long-term average data (320 mm; Fig. 1c). Most of the higher number of rainfall events were located during the spring and autumn seasons, as is typical in this area.

For the evaluation of the ET_o values provided by the non-reference "Ontur" station, the monthly differences of T_{min}—T_{dew} were in general between 1.0 and 7.0 ºC (Fig. 2a), computing values higher than 2 ºC from May to September in all the years studied, and during the winter and autumn months in 2019 and 2022 (data not shown). These conditions were mainly due to a precipitation/ET_o ratio lower than 0.5, which was registered for around 54% of the total analysed months. However, monthly differences for the reference site (Las Tiesas) were lower than 0.6 ºC regardless of the monthly ratio of precipitation to ET_o (Fig. 2a), observing that these differences comprised between 0.4 ºC and 0.6 ºC corresponded to summer months, i.e. when drier conditions occur (precipitation/ET_o ratio < 0.5).

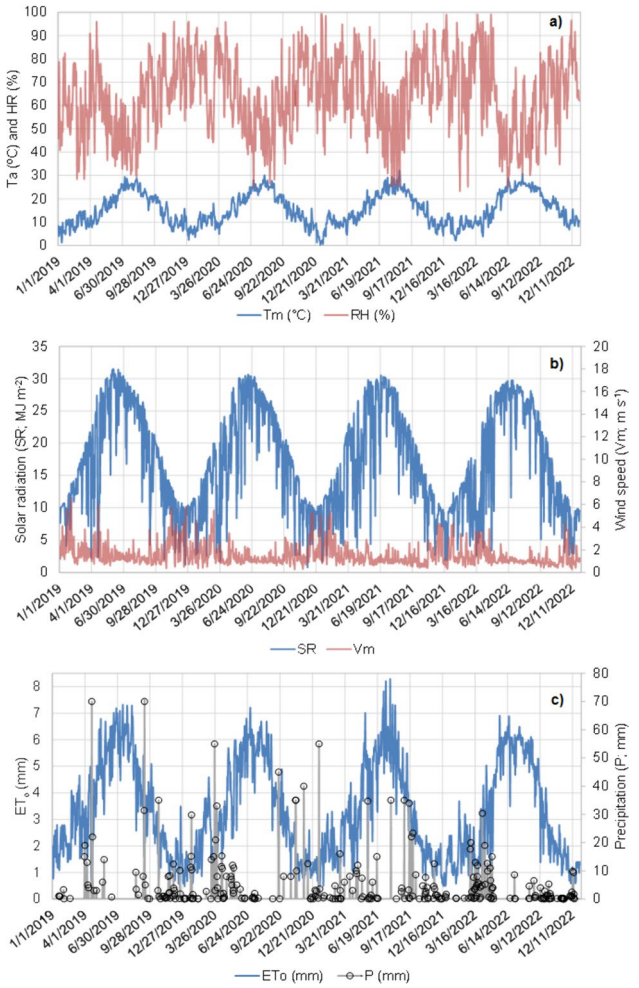

Fig. 1 Daily meteorological data during the almond growing seasons across the four consecutive years of the trial, represented as average daily data for air temperature (Ta) and relative humidity (RH) (a), wind speed and cumulative daily data for solar radiation (b), grass reference evapotranspiration (ET_o) and precipitation (c)

Once T_{max}, T_{min} and T_{dew} were adjusted to the new conditions (Eqs. 2 – 4), the ET_o values (ET_{o_corr}) for this station was newly computed and plotted with respect to the data originally provided by the weather station (ET_o; Fig. 2b). A good significant linear relationship was computed between the two variables, obtaining a very high coefficient of determination ($R^2 = 0.995$), with a slope and y-intercept close to 1.00 and 0.00, respectively (Fig. 2b). Overall, ET_{o_corr} was reduced by around 6% for the four studied seasons. This dataset was used to derive the single and basal almond crop coefficients as ET_c/ET_o and T_c/ET_o, respectively.

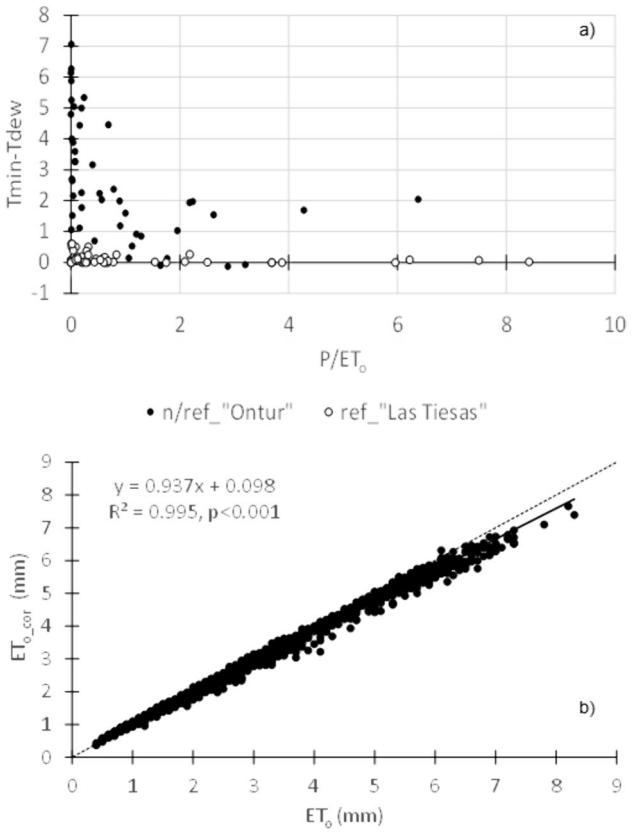

Fig. 2 Comparison of differences between the monthly values of minimum and dew point temperature (T_{min}-T_{dew}) from the reference site (Las Tiesas) and those from the non-reference site (Ontur), with respect to the monthly ratios of precipitation/ET_o (a); and plotted with the ET_o values (ET_o_corr) vs. the former ones calculated by the weather station upon T_{min} T_{max} and T_{dew} having been corrected for the four growing seasons (b). Equation fit, coefficient of determination and significance level are also plotted

Tree determinations and almond production

Overall, the almond phenological stages were not affected by the irrigation systems used in this experiment, with a similar almond tree development being obtained across the four studied seasons (Table 1). The almond trees required around 3,522 ºC of accumulated average thermal time, ranging between 3,436 and 3,644 ºC, to complete the crop cycle length (Table 1). A fair duration of the main phenological stages for almond was obtained in accordance with the coefficient of the variation values reported in Table 1, where a large variability was determined for initial and crop development periods (16.1% and 25.6%, respectively). This variability was lower, however, for the subsequent periods: 3.0% and 10.7%, with mid-season being the most homogeneous period in the area requiring an average value of 2,761 ºC from the swollen bud stage (Table 1). Unlike the other three periods reported in Table 1, crop development was the shortest period in terms of cumulated thermal time, requiring 270

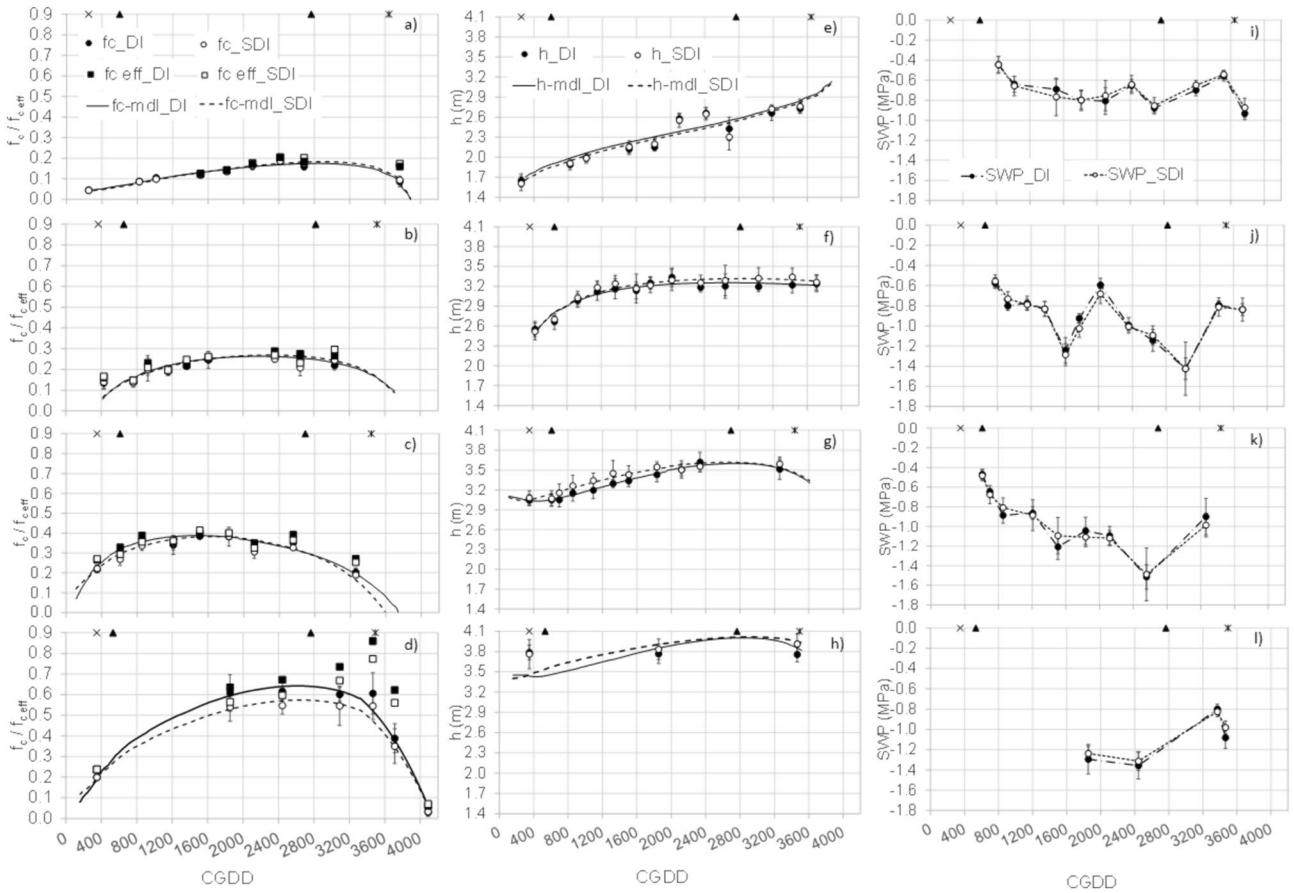

Fig. 3 Seasonal evolution of the fraction ground cover (f_c, circles) and effective f_c ($f_{c\ eff}$, squares) (a, b, c and d), tree height (h, circles) (e, f, g and h), and midday stem water potential (SWP) measured over the four study seasons (2019: a, e and i; 2020: b, f, j; 2021: c, g, k; 2022: d, h, l) as a function of the cumulative growing degree days (CGDD) for surface- and subsurface-drip irrigation systems (DI and SDI, respectively). Vertical bars: standard deviation of the average value; cross symbol: onset of fruit set stage; triangle symbols: onset and end of mid-season period; start symbol: end-season (onset of leaf drop)

ºC as the average value for the four seasons; while initial, mid-season and late stages accumulated 328 ºC, 2,162 ºC and 761 ºC, respectively.

Almond canopy growth, represented in terms of fraction of ground cover (f_c; Figs. 3a–d, circles) and tree height (h; Figs. 3e–h, circles), was positive over the four growing seasons, showing a similar behavior, regardless of the irrigation system considered. The maximum f_c values were 0.19, 0.26, 0.39 and 0.58 in 2019, 2020, 2021 and 2022, respectively. The inter-annual average increase rate for f_c was determined at around 0.13, having minimum and maximum rates of 0.07 and 0.19, while the maximum h values ranged between 2.65 m in 2019 and 3.80 m in 2022. The larger height growth rate was observed between 2019 and 2020 (around 0.75 m), while a steadier rate, around 0.20 m, was obtained for the rest studied seasons. The daily f_c and h evolution modelled to be used by STSEB model are also represented in Figs. 3a–h (continuous and dotted lines for DI and SDI treatments).

The $f_{c\ eff}$ evolution is also plotted across each growing season (Figs. 3a–d; squares). In the four campaigns, f_c and $f_{c\ eff}$ showed a similar evolution pattern, while an increase in both variables was produced, in general terms, until the early hull split stage (around 200 ºC before the end of mid-season; Figs. 3a–d), followed by a decrease, coinciding with the end of mid-season (fruit ripe stage), until complete senescence of the trees. The maximum average $f_{c\ eff}$ values reached 0.20, 0.28, 0.41 and 0.82 in 2019, 2020, 2021 and 2022, respectively. During the mid-season stage, f_c and $f_{c\ eff}$ values were very close, with average differences computed of about 8.0%; whereas the measured values of f_c during the initial and late season stages, and those computed for $f_{c\ eff}$, showed much greater differences (around 60.0%) because of the mean angle of the sun above the horizon during those time periods. These differences were most evident in the 2022 campaign, with average f_c values for both irrigation systems of 0.58 at the end-season stage,

and 0.37 after end-season stage, with computed average $f_{c\ eff}$ values of 0.82 and 0.59, respectively (Fig. 3d).

Tree water status, characterized by the midday stem water potential measurements, ranged between -0.5 MPa and -1.1 MPa over the three first growing seasons during mid-season and post-harvest periods, suggesting the almond trees were in a hydric comfort zone (Figs. 3i–l) (Montoya et al. 2022). Only in the pre-harvest period in the 2020 and 2021 seasons, as well as during mid-season period in 2022, were SWP values of close to −1.5 MPa reached. Like the f_c and h measurements, the SWP values showed a similar trend between the DI and SDI systems over the four studied seasons (non-significant differences).

Finally, kernel yield (Y_k) showed no differences between the two irrigation systems, with values reaching 2200 kg ha^{-1} in the fourth crop-greening (Table 2). However, in the first and third harvest year, Y_k was around 450 kg ha^{-1} and 250 kg ha^{-1}, respectively. The lowest Y_k obtained by the farmer in 2022 was due to a late frost occurring at the onset of the fruit set stage causing a yield reduction in almost 95%.

Irrigation water applied, crop evapotranspiration and E_s/T_c partitioning

In general terms, the irrigation water applied to the crop increased as the tree canopy cover also rose over the four studied seasons. The total irrigation water (IW) depth applied to the DI system ranged between 2,581 m^3 ha^{-1} in 2019 and 7,158 m^3 ha^{-1} in 2021 (Table 2). The SDI system received between 10% less irrigation water in 2019, and around 13.8% less in 2020 and 2021. However, the accumulated IW applied for 2022 was 99 mm and 77 mm less for DI and SDI, respectively, compared with those values for 2021. The highest values of the total IW applied to the almond trees corresponded to the mid-season stage of each growing season (Table 2), which represented around 69% of the total irrigation water due to, on one hand, the duration of this stage was the largest (2,162 ºC) and, on the other hand, it mainly occurring during the summer months (low number of precipitation events and of short depth, and high evaporative demand; Fig. 1c and Table 2). In contrast, during the late stage, the almond trees received around 22% of the total IW as the average value of the four experimental years.

The estimated crop evapotranspiration and its components (E_s and T_c) using STSEB showed a similar behaviour to that described for IW. It is worth highlighting that ET_c and T_c during mid-season were substantial with respect to their accumulated values (Table 2), representing between 42 and 76% for ET_c, and between 72 and 85% for T_c. Excluding the last growing season, where the ET_c and T_c estimations for DI system were not representative for the complete crop cycle (Table 2), total ET_c was notably different between the two irrigation systems (between 12 and 31%), but not so evident in terms of T_c (between 5 and 19%). This was due to the soil evaporation estimates, since the DI system reported larger E_s values than the SDI system during the mid-season stage (Table 2). Moreover, E_s, either estimated by STSEB or calculated by SWB during the mid-season stage, decreased as canopy size rose for both irrigation systems; i.e. changing from 21% higher for DI than SDI in 2019, to only a 3% difference in 2022 in accordance with STSEB estimates. A similar trend for E_s was computed by the SWB approach (Table 2).

Dual crop coefficient ($K_{cb}+K_e$) evolution. Approaches from canopy cover and tree height, and surface energy balance

The K_{cb} seasonal evolution estimated by the A&P approach ($K_{cb\ A\&P}$) and STSEB model ($K_{cb\ STSEB}$) showed a similar behaviour in both irrigation systems over the four experimental years (Figs. 4a-d). The statistical analysis performed for $K_{cb\ A\&P}$ values showed no significant differences between the two irrigation systems for every growing season (Table 3). However, $K_{cb\ STSEB}$ showed some differences between both irrigation systems, being much less significant in the two first seasons than in 2021 and 2022 (Table 3), i.e. 0.02 vs. 0.06 in 2021 and 0.10 in 2022.

Table 4 summarizes the K_{cb} values obtained for both irrigation systems using the A&P approach for the four almond growing seasons, identifying initial, mid- and end- season crop growth stages, following the FAO56 approach (Allen et al. 1998; Pereira et al. 2021a). $K_{cb\ A\&P}$ was computed considering the average values of both $f_{c\ eff}$ as f_c (circles and squares, respectively; Figs. 4a–d). Thus, the maximum values of $K_{cb\ A\&P}$ were reached during mid-season ($K_{cb\ mid}$) coinciding with the highest values of both $f_{c\ eff}$ or f_c and h (Figs. 4a–d; Table 4). However, $K_{cb\ A\&P}$ for the end-season ($K_{cb\ end}$) was represented by tree conditions prior to leaf drop (i.e. at full maturation of both flowering and vegetative buds), with f_c between 0.07 and 0.12 lower than their maximum values (Figs. 3a,b,d), excepting 2021, for which the difference was 0.22 (Fig. 3c) due to a rapid leaf drop caused by incorrect leaf micronutrient application during the post-harvest period. The $K_{cb\ A\&P}$ estimates data using M_L and F_r values parameterized by López-Urrea et al. (2024) and $f_{c\ eff}$ showed to be slightly higher to those estimations obtained by STSEB across the four growing seasons (Figs. 4a–d). These overestimations are highlighted during mid-season in the first and last season, and during post-harvest period for all growing seasons (differences ranging between 0.05 and 0.25). Both fractions ($f_{c\ eff}$ or f_c) used to calculate $K_{cb\ A\&P}$ reported similar crop coefficients for almost all the crop cycle, resulting between 0.03 and 0.17 higher for $f_{c\ eff}$ than f_c (Figs. 4a–d). In general terms, the lowest differences were

Table 2 Accumulated values of ET_o, water received (Pe and IWA) by the crop, soil evaporation (E_s), crop transpiration (T_c) and crop evapotranspiration (ET_c) relative to the growth stages for the period of time constrained to the availability of radiometric thermal measurements for the two drip irrigation systems (DI and SDI). Commercial kernel yield is also shown for every growing season

Season	Growth stage	ET_o (mm)	Pe (mm)	IWA (mm)		E_s_SWB (mm)		E_s_STSEB (mm)		T_c_STSEB (mm)		ET_c_STSEB (mm)		Y_k (kg ha^{-1})	
				DI	SDI	DI	SDI	DI	SDI	DI	SDI	DI	SDI	DI	SDI
2019	Initial	–	–	–	–	–	–	–	–	–	–	–	–	–	–
	Crop development	109.5	93.3	9.8	9.8	33.9	31.3	32.3	33.1	4.1	3.4	36.7	36.5		
	Mid-season	623.0	22.1	174.8	156.3	65.3	13.1	30.0	4.2	98.6	84.1	128.5	88.2		
	Late	163.8	130.6	43.1	41.5	25.0	16.4	21.3	29.2	31.9	28.6	53.4	57.8		
	Accumulated	896.3	246.1	227.7	207.6	124.1	60.9	83.7	66.4	134.6	116.1	218.6	182.5		
		(1078.1)	(289.2)	(258.1)	(232.4)	(150.2)	(79.2)	–	–	–	–	–	–		
2020	Initial	–	–	–	–	–	–	–	–	–	–	–	–	480	412
	Crop development	–	–	–	–	–	–	–	–	–	–	–	–		
	Mid-season	462.8	0.0	300.5	258.0	38.8	0.4	40.7	13.6	183.3	173.3	223.9	196.6		
	Late	162.2	46.3	88.5	74.7	20.9	13.9	40.0	35.6	44.1	39.6	84.0	80.4		
	Accumulated	625.0	46.3	388.5	332.6	59.7	14.4	80.8	49.2	227.4	212.9	307.9	277.0		
		(1075.7)	(341.8)	(518.8)	(446.8)	(172.2)	(109.5)	–	–	–	–	–	–		
2021	Initial	101.3	21.6	21.6	19.9	32.4	23.0	12.0	10.6	1.3	1.2	13.8	12.6	2206	2163
	Crop development	87.8	34.4	30.9	25.8	18.1	10.8	21.6	17.9	28.8	23.3	51.2	41.7		
	Mid-season	675.7	90.7	503.1	428.9	108.4	34.0	103.8	69.1	332.9	268.1	446.2	325.4		
	Late	154.0	117.6	113.1	120.4	39.5	35.1	44.6	38.1	30.3	27.2	76.4	67.3		
	Accumulated	1054.8	264.3	678.4	594.9	198.4	102.9	182.1	135.7	393.2	319.8	587.7	447.0		
		(1141.9)	(287.5)	(715.8)	(617.4)	(210.8)	(111.4)	–	–	–	–	–	–		
2022	Initial	69.9	88.4	8.9	8.9	41.7	41.3	21.5	21.1	3.9	6.7	25.4	27.8	261	239
	Crop development	72.2	71.9	4.0	4.0	26.4	26.5	28.4	27.7	20.4	20.7	48.7	48.4		
	Mid-season	722.7	45.4	415.6	360.4	19.8	20.6	84.8	75.3	107.0*	397.9	153.0*	473.1		
	Late	162.5	3.8	138.7	122.7	2.5	2.9	45.1	49.5	89.1	89.9	134.2	139.4		
	Accumulated	1027.2	225.4	567.1	496.0	90.5	91.3	179.8	173.6	220.4*	515.1	361.4*	688.7		
		(1195.3)	(225.4)	(616.9)	(540.4)	(112.3)	(112.7)	–	–	–	–	–	–		

ET_o reference evapotranspiration after correction of weather data observed in non-reference site, Pe effective precipitation, IWA irrigation water applied, E_s soil evaporation, T_c crop transpiration, ET_c crop evapotranspiration, SWB soil water balance, STSEB simplified two-source energy balance, Y_k total kernel yield (7% moisture content)

Values between brackets represent the total accumulated for the complete almond tree cycle from swollen buds to the complete leaf drop

* time series not completely monitored

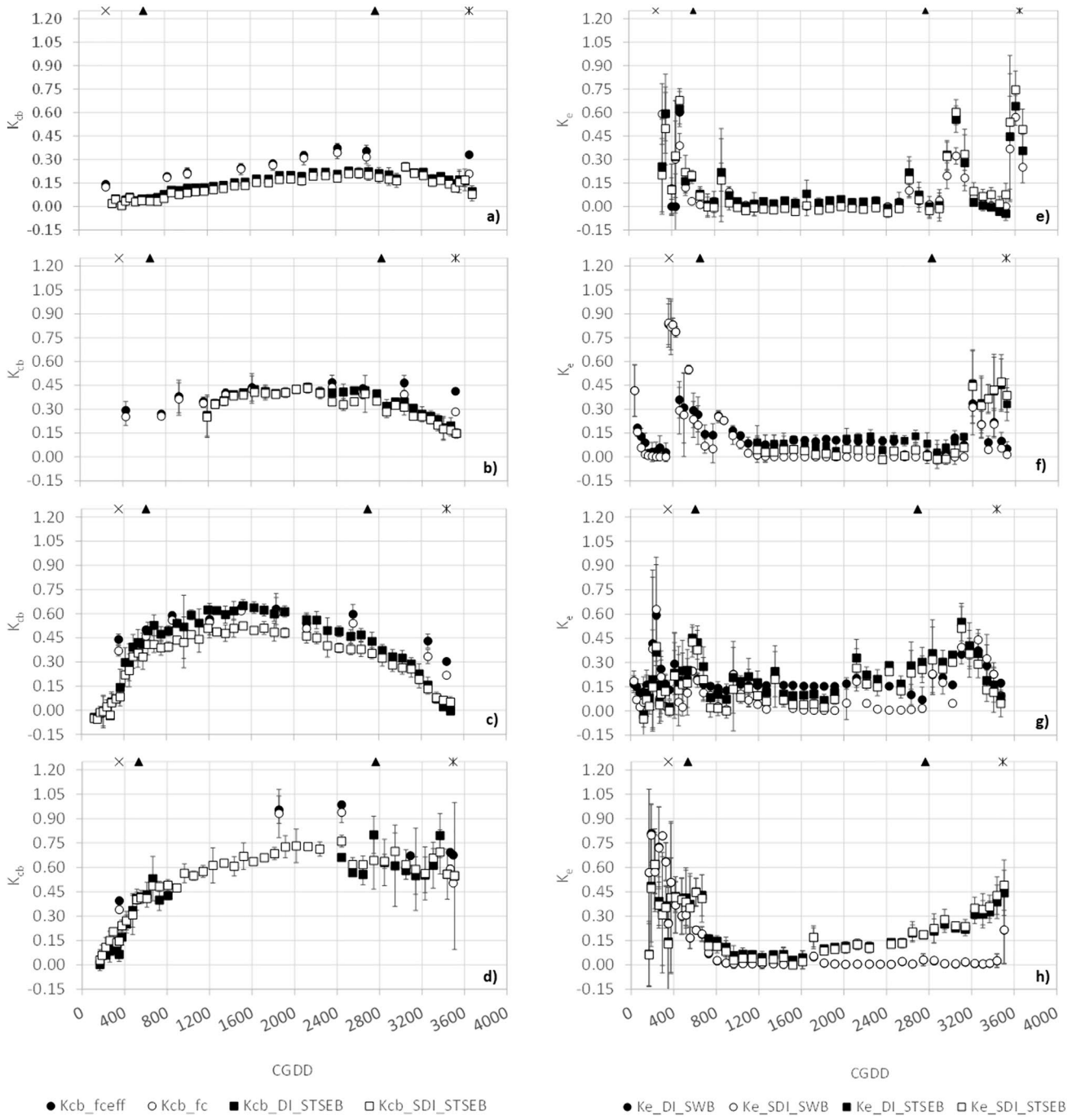

Fig. 4 Seasonal evolution of the basal crop coefficient (K_{cb}) and soil evaporation coefficient (K_e) as a function of the cumulative growing degree days (CGDD) for the surface- (DI) and subsurface-drip (SDI) irrigation systems across the four studied seasons (2019: a and e; 2020: b and f; 2021: c and g; 2022: d and h). Vertical bars: standard deviation of the average value every five days; cross symbol: onset of fruit set stage; triangle symbols: onset and end of mid-season period; start symbol: end-season (onset of leaf drop)

Table 3 Comparison of means (ANOVA test) and medians (Wilcox test) for K_c, K_{cb} and K_e estimated by the STSEB model and calculated using the A&P approach (K_{cb}), and soil water balance (K_e) (SWB)

Season	Model	Coef	Irrigation system	S-W	Bt	ANOVA	M-W
2019	A&P + SWB	K_{cb}	DI	ns	ns	ns	–
			SDI	ns			
		K_e	DI	***	ns	–	***
			SDI	***			
	STSEB	K_{cb}	DI	***	ns	–	*
			SDI	***			
		K_e	DI	***	*	–	ns
			SDI	***			
2020	A&P + SWB	K_{cb}	DI	ns	ns	ns	–
			SDI	ns			
		K_e	DI	***	ns	–	***
			SDI	***			
	STSEB	K_{cb}	DI	***	ns	–	*
			SDI	***			
		K_e	DI	***	ns	–	***
			SDI	***			
2021	A&P + SWB	K_{cb}	DI	*	ns	–	ns
			SDI	**			
		K_e	DI	***	**	–	***
			SDI	***			
	STSEB	K_{cb}	DI	***	***	–	***
			SDI	***			
		K_e	DI	***	ns	–	***
			SDI	***			
2022	A&P + SWB	K_{cb}	DI	ns	ns	ns	–
			SDI	ns			
		K_e	DI	**	ns	–	ns
			SDI	**			
	STSEB	K_{cb}	DI	***	*	–	***
			SDI	***			
		K_e	DI	**	ns	–	***
			SDI	***			

S-W normality (Shapiro Wilk test), *Bt* homoscedasticity (Barlett test), *ANOVA* analysis of variance, *M-W* median comparison test (Mann–Whitney: Wilcox test), *DI* surface drip irrigation system, *SDI* subsurface drip irrigation system

p-value: level of significance (ns: not significant; *: $0.05 > p > 0.01$; **: $0.01 > p > 0.001$; ***: $p < 0.001$)

observed during mid-season for all years (< 0.05), while the largest were identified as late stage was ending, with the differences ranging between 0.08 and 0.17. $K_{cb\ ini}$, $K_{cb\ mid}$ and $K_{cb\ end}$ increased every year (from the second to fifth crop-greening) as $f_{c\ eff}$ or f_c values became higher (Figs. 4a–d). Considering $f_{c\ eff}$, the average $K_{cb\ A\&Pmid}$ was 0.30, 0.39, 0.60 and 1.00 for the 2019, 2020, 2021 and 2022 campaigns, corresponding to $f_{c\ eff}$ values of 0.15, 0.26, 0.37, and 0.62, respectively (Fig. 4; Table 4).

The evolution of the soil evaporation coefficient computed through SWB ($K_{e\ SWB}$; circles in Figs. 4e–h) and estimated from STSEB ($K_{e\ STSEB}$; squares in Figs. 4e–h) showed a similar trend across the four experimental seasons, ranging between values as large as 0.90, due to rainfall events at crop development and post-harvest stages when the ground cover values were low, to minimum values of 0.05 or less, mainly calculated and estimated during the mid-season stage (Figs. 4e–h; Table 4). In addition, both approaches reported around 16% higher K_e values for DI than SDI during the four experimental seasons. These average differences between the two irrigation systems were clearly identified through the statistical analysis performed for each growing season, where both approaches showed that K_e was significantly different between DI and SDI for almost all the growing seasons (Table 3).

Table 4 Summary of observed and standard crop coefficients (K_{cb}, K_e and K_c) relative to the initial, mid- and end-season periods, computed with the A&P approach in accordance with the effective fraction canopy cover ($f_{c\ eff}$), tree height (h), and M_L and F_r values tabulated by López-Urrea et al. (2024). Statistical indicators evaluate the goodness of fit of the crop coefficients between those computed by the A&P approach (K_{cb}) + soil water balance (K_e), and those estimated through the STSEB model

Season	Growth stage / statistical indicators	h (m) (range)	$f_{c\ eff}$ (range)	M_L	F_r	Observed crop coefficients					Standard crop coefficients		
						K_{cb} (range)	K_e~		K_c		K_{cb}	K_c	
							DI	SDI	DI	SDI		DI	SDI
2019	Initial	1.63	0.06	1.5	1.00	0.15	0.33	0.31	0.48	0.46	0.15	0.48	0.46
	Mid-season	2.36 (2.00–2.65)	0.15 (0.09–0.20)	1.3	1.00	0.28 (0.19–0.37)	0.10	0.02	0.38	0.30	0.28	0.38	0.30
	End-season	2.72	0.22	1.1	1.00	0.33*	0.20	0.16	0.53	0.49	0.33*	0.53	0.49
	RMSE	–	–	–	–	0.15	0.10	0.11	0.18	0.16	–	–	–
	MBE	–	–	–	–	0.15	0.03	–0.02	0.18	0.15	–	–	–
	d	–	–	–	–	0.88	0.96	0.96	0.85	0.89	–	–	–
2020	Initial	2.54	0.16	1.5	0.85	0.29	0.18	0.15	0.47	0.44	0.29	0.47	0.44
	Mid-season	3.10 (2.65–3.35)	0.23 (0.20–0.29)	1.7	0.75	0.39 (0.27–0.47)	0.11	0.04	0.50	0.43	0.39	0.50	0.43
	End-season	3.27	0.24	1.7	0.75	0.41*	0.12	0.08	0.53	0.49	0.41*	0.53	0.49
	RMSE	–	–	–	–	0.13	0.28	0.28	0.41	0.40	–	–	–
	MBE	–	–	–	–	0.10	0.11	0.08	0.24	0.20	–	–	–
	d	–	–	–	–	0.90	0.69	0.72	0.43	0.47	–	–	–
2021	Initial	3.06	0.27	1.5	0.85	0.44	0.24	0.17	0.69	0.62	0.44	0.69	0.62
	Mid-season	3.35 (3.05–3.62)	0.37 (0.29–0.42)	1.7	0.75	0.61 (0.52–0.67)	0.16	0.06	0.77	0.67	0.56	0.72	0.62
	End-season	3.56	0.18	1.7	0.75	0.31*	0.26	0.26	0.74	0.69	0.31*	0.74	0.69
	RMSE	–	–	–	–	0.20	0.11	0.12	0.24	0.24	–	–	–
	MBE	–	–	–	–	0.17	0.01	–0.02	0.13	0.18	–	–	–
	d	–	–	–	–	0.91	0.93	0.94	0.85	0.85	–	–	–
2022	Initial	3.77	0.24	1.4	0.85	0.40	0.63	0.62	1.03	1.02	0.40	1.03	1.02
	Mid-season	3.80 (3.77–3.85)	0.62 (0.56–0.67)	1.5	0.90	1.02 (0.97–1.05)	0.04	0.04	1.06	1.06	0.97	1.01	1.01
	End-season	3.80	0.72	1.4	0.60	0.67*	0.03	0.04	0.70	0.71	0.67*	0.70	0.71
	RMSE	–	–	–	–	0.24	0.20	0.21	0.50	0.26	–	–	–
	MBE	–	–	–	–	0.22	–0.07	–0.06	0.19	–0.01	–	–	–
	d	–	–	–	–	0.87	0.89	0.89	0.89	0.96	–	–	–

~ average value for late stage

* K_{cb} prior to leaf drop (i.e. onset of leaf drop)

A&P approach assessment

In the 2020 and 2021 experimental seasons, $K_{cb\ A\&P}$ during the mid-season stage showed an excellent agreement with the $K_{cb\ STSEB}$ values estimated every five days (differences between 0.01 and 0.05), with either $f_{c\ eff}$ or f_c being used (Figs. 4b–c). However, in 2019 and 2022, K_{cb} differences were more significant during mid-season growth stage, ranging from 0.13 in 2019 (Fig. 4a) to 0.40 in 2022 (Fig. 4d). Moreover, this was also identified during the late stage; $K_{cb\ A\&P}$ values determined using $f_{c\ eff}$ tended to be much higher, between 0.06 and 0.18, than the $K_{cb\ A\&P}$ values obtained through f_c (between 0.01 and 0.08), with regard to the $K_{cb\ STSEB}$ estimations. Overall, $K_{cb\ A\&P}$ and $K_{cb\ STSEB}$ showed a very good agreement ($0.80 < d < 0.98$; Table 4) despite $K_{cb\ A\&P}$ overestimating $K_{cb\ STSEB}$ at an average value of 0.16 or 0.10 when using $f_{c\ eff}$ or f_c, respectively (Figs. 4a–d). Additionally, the two $K_{cb\ A\&P}$ datasets estimated either using $f_{c\ eff}$ or f_c (Figs. 4a–d), together with those $K_{cb\ STSEB}$ values, showed high coefficients of determination ($R^2 > 0.80$) for the linear regressions associated with the Deming method. These regressions attained similar slopes (around 0.86) and intercepts of 0.18 and 0.14 for $f_{c\ eff}$ and f_c, respectively (Fig. 5). A lower intercept was reached using f_c because better fits to the STSEB estimates were mainly obtained during late season stage (Figs. 4a–d).

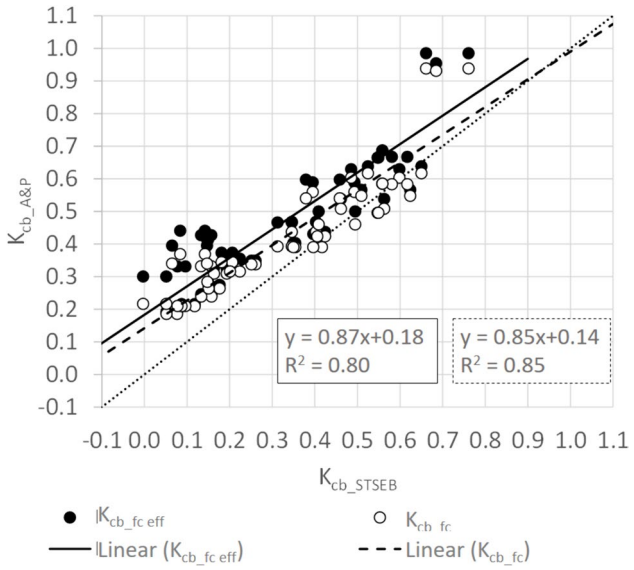

Fig. 5 Relationship between average basal crop coefficients values estimated by the A&P approach and STSEB model, considering both $f_{c\ eff}$ (black circles) as f_c (white circles) in the A&P approach equations (color figure online)

The average K_e computed by the SWB tended to underestimate that obtained from the STSEB approach, with errors of around 0.20 for both irrigation systems (Table 4). These errors represent between 0.7 mm and 1.5 mm when the highest ET_o values are considered. The index of agreement between $K_{e\ SWB}$ and $K_{e\ STSEB}$ for the four seasons was, in general, good, attaining the best fits ($d \approx 0.94$) and the lowest errors (RMSE ≈ 0.11) in 2021 (Table 4). However, somewhat higher errors and moderate fits were obtained in 2020 (RMSE ≈ 0.28, $d \approx 0.70$; Table 4).

Finally, the average K_c values reported in this research showed an inter-annual increase as $f_{c\ eff}$ / f_c and h also rose (Table 4). As for $f_{c\ eff}$, $K_{c\ A\&P+SWC}$ for the mid-season ($K_{c\ mid}$) ranged from 0.30 in 2019 to 1.06 in 2022. However, the average $K_{c\ A\&P+SWC}$ for the initial stage ($K_{c\ ini}$) and end-season ($K_{c\ end}$) moved in the same ranges as $K_{c\ A\&P+SWC\ mid}$ for every growing season, with these differences being in the order of 0.05–0.19 for the first season and of around 0.05 for the rest of seasons, excepting in 2022, when there was a difference of around 0.40 between $K_{c\ A\&P+SWC\ mid}$ and $K_{c\ A\&P+SWC\ end}$ (Table 4). Overall, $K_{c\ A\&P+SWB}$ overestimated $K_{c\ STSEB}$ with larger errors (around 0.26) than those obtained in the K_{cb} (Table 4). Evidently, the different $K_{c\ A\&P+SWB}$ values estimated for DI and SDI were due to the computed $K_{e\ SWB}$ ranges.

Standard crop coefficients

After adjusting local climatic conditions to the standard conditions (i.e. u_2: 2 m s^{-1}; RH_{min}: 45%), $K_{cb\ A\&P}$ for the mid- and end- seasons of 2021 and 2022 were corrected, since the estimated $K_{cb\ A\&P}$ values were higher than 0.45 (Table 4). This adjustment to the standard conditions led to $K_{cb\ A\&P\ mid}$ and $K_{cb\ A\&P\ end}$ decreasing between 0.02 and 0.05 (Table 4). Consequently, $K_{c\ A\&P+SWC\ mid}$ and $K_{c\ A\&P+SWC\ end}$ for both seasons were also modified in the same range (Table 4).

Discussion

ET_o after correction of weather data

The general tendency of monthly T_{min} values above T_{dew} values for both reference (Las Tiesas) and non-reference (Ontur) sites obtained in this study was also observed by Allen (1996) comparing two semiarid locations in Idaho (US) 200 km apart. This author obtained differences as high as 10 ºC for the non-reference site, and between 2 ºC and 5 ºC for the irrigated site, having a close relationship to the precipitation/ET_o ratio where values lower than 0.5 showed high aridity in its study area, causing the T_{min}-T_{dew} difference to exceed 2 ºC in most cases. Similarly, this relationship is consistent with findings for the most inland areas of Spain; De La Antonia Gonzalez (2023) obtained, for Albacete station (area influence of the present research) and other locations, T_{min}-T_{dew} differences higher than 2 ºC and precipitation/ET_o ratio lower than 0.5 over four and seven successive months, respectively, indicating high aridity conditions during the warm season and the bordering months. Aridity conditions during those months of winter and autumn of 2019 and 2022, respectively, are shown by the low number of precipitation events and total rainfall amount registered in the area, i.e. 7 mm and 40 mm, respectively when the accumulated ET_o is typically similar (Fig. 2c). The general reduction in the ET_o with respect to ET_o for the Ontur weather station has also been observed for weather stations located under similar conditions in northeast Spain, where slopes between ET_o values after being corrected and non-corrected the weather data differed by around 3.5% (De La Antonia Gonzalez 2023). The reduction of around 6% in ET_o due to aridity conditions computed in this research can be not much relevant towards the estimated crop coefficients. However, the aridity conditions in other productive areas in the world can be much stronger, making the correction of weather data a step required for estimating properly the crop water requirements.

Almond growth stages related to cumulative growing degree days and tree determinations

The variability in cumulative growing degree days (CGDD) reported in Table 1 was similar to, and even lower than, the values computed with other crops typically grown in the area, such as maize (Domínguez et al. 2012b) and onions (Domínguez et al. 2012a), where the higher and lower variability identified by those authors was at initial and development stages (between 11.5% and 17.7%) and the late stage (between 4.6% and 7.5%). The average CGDD values for mid-season in this research (i.e. 2,162 ºC; Table 1) coincide with those reported by Paredes et al. (2024a) for almond tree of early maturation (close to 2250 ºC). Similar differences are observed for the rest of growth stages, being 74 ºC, 35 ºC and 59 ºC for initial, growth development and end-season stages, respectively.

The threshold temperatures considered in this work, i.e. T_{base} of 4.5 ºC and T_{upper} of 35 ºC, differed slightly to the values used by Lorite et al. (2020) (T_{base} of 4 ºC and T_{upper} of 36 ºC) to identify, through a modelling framework, the flowering date of several almond cultivars in different areas of the Iberian Peninsula. However, their cultivars did not include Penta. Nevertheless, these authors determined that the day of year for the start of full bloom, for late-flowering cultivars (e.g. cv. "Lauranne"), was around 70, with an inter-annual standard deviation of around 7.5 and 10.9 days for different places in the Iberian Peninsula. Taking into account that the full bloom stage for Lauranne is around 6–10 days earlier than Penta in the area (F. Mañas, personnel communication), these dates agree with the results shown in Table 1, where day of year 88 was the average value reported for the full bloom stage using the 4 studied seasons. Note that the lacks of studies related with extra-late flowering cultivars like Penta, in terms of accumulated thermal time for each phenological stage.

A detailed description and analysis of the variables related to canopy growth for the three first study campaigns is included in Montoya et al. (2022). In summary, the statistical analysis carried out by these authors evidenced that the irrigation system used, and the irrigation water applied, did not influence the tree behaviour in terms of f_c and h. Similar conclusions can be extracted for the last study season, since the measured f_c and h showed no significant differences between the two irrigation systems (Figs. 3d , h; statistical analysis results are not shown).

In general terms, the optimal agricultural management in this experimental almond orchard led f_c to almost triple from a young age (second crop-greening) to mature age (fifth crop-greening). Despite the f_c evolution in 2021 being characterized by its rapid drop during the late stage, as Montoya et al. (2022) reported, the f_c inter-annual increase rate between 2020 and 2021 almost doubled with respect to the previous season, i.e. 0.13 vs. 0.07 obtained between 2019 and 2020; while that inter-annual rate for the following two seasons was 0.19, which is around 50% higher. Considering the same tree ages as in this research, several authors have found similar values for f_c inter-annual changes. Drechsler et al. (2022) reported changes of 0.16 and 0.08 in two 2 to 3 year-old and 4– 5 year old almond orchards, respectively; Sánchez et al. (2021) identified a change of 0.15 and 0.05 between the third and fourth crop-greening and between the fourth and fifth crop-greening, respectively; while more uniform f_c inter-annual changes, between 0.10 and 0.15, were observed by Espadafor et al. (2015) across the first four years after planting a 'Guara' almond orchard. In contrast to the f_c tendency observed in this experiment, which started to decline at the end of August (close to harvest date; Figs. 3a–d), Espadafor et al. (2015) showed a much more uniform ground cover tendency. Regarding tree height evolution measured in this experiment (Figs. 3e–h), the values are consistent with the data reported by Quintanilla-Albornoz et al. (2023) and the classification provided by López-Urrea et al. (2024) after a comprehensive literature review to update K_c and K_{cb} values for almond trees. For a training system based on open vase, López-Urrea et al. (2024) proposed a range of h and f_c of 4.0–4.5 m and 0.40–0.55, respectively, being similar to the maximum values of this research.

Like the findings for f_c and h, SWP showed no significant dependence on the irrigation system. In accordance with Fulton et al. (2014), the total amount of water applied by both irrigation systems led the almond trees to be well-watered for almost the whole growing cycle. However, moderate stress (values of SWP close to −1.5 MPa) was identified in 2020 and 2021 over a short period of time located at pre-harvest because it is a common agronomic practice to suppress or reduce irrigation in that period to avoid or minimize the risk of bark splitting during the harvesting process. Tree water stress was also observed for days close to harvest time by Drechsler et al. (2022), albeit with the midday SWP falling towards values as deep as −3.1 MPa. Likewise, moderate stress conditions were also maintained during the mid-season period in 2022 because of the late frost occurring at the onset of fruit set stage. This was the cause of the lack of kernel yield in 2022 (Table 2). Reasons such as seeking to avoid very vigorous tree canopy growth, together with an imbalance of the economical revenues, led the farmer to decide to apply moderate water deficit conditions, mainly during the mid-season stage (Fig. 3l). In this sense, the total irrigation water applied in 2022 was around 13% less than in 2021 (Table 2), when the total effective precipitation in the crop cycle was also lower (21.6% less). Nonetheless, canopy growth continued to increase, since almost its total crop water requirements were met, either by irrigation, precipitation or the soil water reserve, as previously described.

Table 5 Characteristics of the almond fruit orchards and its crops coefficients derived from field observations both from several study sites as in this experiment

Author	Age (years)	f_c or f_{ceff}	h (m)	Crop coefficients from field observations					
				$K_{cb\ ini}$	$K_{cb\ mid}$	$K_{cb\ end}$	$K_{c\ ini}$	$K_{c\ mid}$	$K_{c\ end}$
Drechsler et al. (2022)	1	n/r	2.0	n/r	n/r	n/r	n/r	0.40	0.20
	2	0.09	3.0	n/r	n/r	n/r	n/r	0.50	0.20
	3	0.23–0.25	4.0	n/r	n/r	n/r	0.40	0.80–0.90	0.45
	4	0.22–0.47	4.0–5.0	n/r	n/r	n/r	0.50	0.90–1.10	0.40
	5	0.55	5.0	n/r	n/r	n/r	0.45	1.00	n/r
Espadafor et al. (2015)	3	0.36	n/r	0.30	0.50	0.18	n/r	n/r	n/r
	4	0.48	4.8	0.15	0.55	0.40	n/r	n/r	n/r
García-Tejero et al. (2015)	4	n/r	n/r	n/r	n/r	n/r	0.40	1.10	0.50
López-López et al. (2018)	5	0.55	n/r	0.30	0.65	0.50	n/r	n/r	n/r
	6	0.59	n/r	0.15	0.80	0.60	n/r	n/r	n/r
	7	0.55	n/r	n/r	0.95	0.70	n/r	n/r	n/r
Ramos et al. (2023)	5–6	0.41	4.0	0.22	0.58	0.50	0.99	0.65	0.96
Sánchez et al. (2021)	2	0.21	1.8	n/r	0.19	n/r	n/r	0.30	n/r
	3	0.35	3.0	n/r	0.30	n/r	n/r	0.33	n/r
	4	0.39	3.8	n/r	0.36	n/r	n/r	0.45	n/r
In this study	2	0.15	2.4	0.15	0.28	0.33	0.48~	0.38~	0.53~
							0.46*	0.30*	0.49*
	3	0.23	3.1	0.29	0.39	0.41	0.47~	0.50~	0.53~
							0.44*	0.43*	0.49*
	4	0.37	3.4	0.44	0.61	0.31	0.69~	0.77~	0.74~
							0.62*	0.67*	0.69*
	5	0.62	3.8	0.40	1.02	0.67	1.03~	1.06~	0.70~
							1.02*	1.06*	0.71*

~ K_c estimated for surface drip irrigation system (DI)

* K_c estimated for sub-surface drip irrigation system (SDI)

In this regard, there is a gap in the literature on how to manage irrigation water in an almond orchard (total volume applied and allocation along the season), and the effects on the subsequent season when the fruit load is minimum due to climatic effects such as those in 2022. Works have reported that the transpiration rate of the almond tree decreased during mid-season because of a low fruit load in comparison to a previous year with a higher load (differences of kernel yield not reported; Espadafor et al. 2015); in the case of apple and pear, the evapotranspiration rate also diminished after fruit removal at harvest (Girona et al. 2011; Auzmendi et al. 2011).

Evapotranspiration and crop coefficients for young almond trees

The analysis of the total net water available for the crop (Pe + IWA; Table 2) for both irrigation systems showed that the largest differences were mainly observed during mid-season, attaining values between 9.4% and 14.1% higher for DI than SDI. Clearly, as the cumulative Pe during spring and autumn seasons was larger than for summer, irrigation requirements were lower, and therefore, differences between irrigation systems were not noteworthy (around 4%). This difference between the two irrigation systems is consistent, despite the lower amount of water used in 2022. Broadly speaking, the total IW applied in this research was close to the amount of water used by Quintanilla-Albornoz et al. (2023). Drechsler et al. (2022) and Sánchez et al. (2021), considering the same range of f_c although tree age can differ. Comparing ET_c and T_c estimations with STSEB model between the different growing seasons, it is observed that the increase in the size of the canopies also involved a raise value for both variables, while E_s tended to decrease in the growth stages which were completely monitored (mainly mid- and late-season; Table 2; Figs. 3a–d). In addition, the total crop evapotranspiration estimates with STSEB model for the completely monitored growth stages of 2021 and 2022 (Table 2) coincide with the different TSEB estimations for mature almond trees reported by Quintanilla-Albornoz et al. (2023), who separated the soil evaporative component to the tree transpiration component.

The lack of evidence that the intra-annual $K_{cb\ A\&P}$ evolution was significantly influenced by the irrigation system, allows us to affirm that a single $K_{cb\ A\&P}$ for every growth stage and age tree can be proposed. This behavior is logical since no significant differences in terms of f_c/$f_{c\ eff}$, and h evolution (Figs. 3a–h) were observed between the two irrigation systems for any growing season (Montoya et al. 2022). Meanwhile, the slight statistical differences found in $K_{cb\ STSEB}$ between DI and SDI in 2019 and 2020 (i.e. 0.02) could be omitted taking into account the criteria used to tabulate K_c and K_{cb} values for fruit orchards (Allen and Pereira 2009; Pereira et al. 2023; López-Urrea et al. 2024; Paredes et al. 2024b), where changes in K_c/K_{cb} every 0.05 were established assuming that change as the error derived using this approach, similarly to the ± 10% considered by Rallo et al. (2021) on the indicative standard values of K_c and K_{cb}. In this sense, and in accordance with the f_c evolution and the SWP measured over both seasons (Figs. 3a,b,i,j), it is reasonable to think that the average K_{cb} of both irrigation systems, obtained for those two years, can be indicative values for young almond trees ($f_c < 0.30$ and $h < 3.0$ m) or with low degree of ground cover ($0.20 < f_c < 0.40$ and $2.0 < h < 4.0$ m) (López-Urrea et al. 2024).

Determinations of K_{cb} using the A&P approach were carried out in this work considering both $f_{c\ eff}$, as stipulated by the authors that developed this approach, and f_c, since it represents field data unaffected by the solar elevation angle and much easier to measure at any time of the day (Figs. 4a–d) (Pereira et al. 2023). During the mid-season stage, daily $f_{c\ eff}$ and f_c values were close, computing $K_{cb\ A\&P}$ values slightly higher than those reported by Espadafor et al. (2015) ($K_{cb\ mid}$ of 0.13 and 0.60 in the second and the fifth crop-greening, respectively), or by Sánchez et al. (2021), Ramos et al. (2023) and Rallo et al. (2021) under different cropping conditions and almond varieties. Moreover, the standard K_{cb} in this study (Table 4) comprises similar results to those reported for a mature almond orchard (6–9 years after transplanting) by López-López et al. (2018), who proposed a K_{cb} between 0.9 and 1.05 with a f_c of 0.75. During the 2022 mid-season, K_{cb} estimated by STSEB was around 0.60, similar to findings obtained by Espadafor et al. (2015) or by López-López et al. (2018) with a f_c between 0.55 and 0.59, but notably different to the results under the A&P approach (between 0.95 and 1.03; Table 4). $K_{cb\ A\&P}$ values, unlike $K_{cb\ STSEB}$, do not identify water stress conditions. It was the main reason of the former differences found in that year, where a moderate water deficit was triggered (Fig. 3-l) because of almost null kernel yield. In this sense, had the almond tree been managed under well-watered conditions, as for the three previous growing seasons (Figs. 3i–k), a better fit between the two approaches would have been obtained in terms of $K_{cb\ mid}$ derived. In any event, $K_{cb\ A\&P}$ results for initial, mid- and end- seasons, using $f_{c\ eff}$ and the same values of the M_L and F_r variables tabulated by López-Urrea et al. (2024), were in the range of those observed as well as close to the values proposed by the same authors. A comparison among the results obtained in this study and those reported by several authors is shown in Table 5.

In contrast, from the onset of autumn, $f_{c\ eff}$ was markedly higher than f_c (Figs. 3a–d) causing large $K_{cb\ A\&P}$ values (Figs. 4a–d) for the same tabulated M_L and F_r values (Table 4). López-Urrea et al. (2024) tabulated M_L and F_r variables using f_c instead of $f_{c\ eff}$ to derivate K_c and K_{cb} for almond trees. Pereira et al. (2020b) also carried out the prediction of crop coefficients using f_c in vineyards and olive trees. This procedure can be justified when $K_{cb\ A\&P\ mid}$ is computed, since $f_{c\ eff}$ and f_c are reasonably similar at solar noon, as is shown by the results of this research (Figs. 4a–d). In the case of $K_{cb\ A\&P\ ini}$ and $K_{cb\ A\&P\ end}$, its differences between being calculated through $f_{c\ eff}$ or f_c vary somewhat compared to those obtained for $K_{cb\ A\&P\ mid}$, with better fits to those $K_{cb\ end}$ values estimated through STSEB when f_c is used in the A&P approach than $f_{c\ eff}$ (Figs. 4a–d and Fig. 5).

The lack of significant differences between irrigation systems for K_e in 2019 and 2022 for STSEB and SWB, respectively, can be explained by the different degree of f_c attained by the crop and the soil temperature measured by the thermoradiometers. In the first case, a very low f_c generated to a short shaded area by the tree, as well as the low amount of water applied in each irrigation event (Montoya et al. 2022), led the thermoradiometers to monitor similar values of soil temperature in both irrigation systems; in the second case, the large f_c values attained by the tree (around 0.55) did not generate differences in the shaded and irrigated area under the tree, calculating similar soil evaporation using the SWB model (Allen et al. 2005). Despite the STSEB and SWB models are conceptually different (STSEB based on the surface energy balance whereas SWB is a soil water balance), and SWB shows somehow more simplicity than STSEB since it does not need to be fed with continuous measurements of soil surface temperature, statistical indicators comparing both models have shown errors acceptable deviations, with similar tendencies of K_e values along the intra- and inter- annual estimates. In addition, the uncertainty associated to both models is very similar in both studied irrigation systems, with every rainfall or irrigation event affecting the same.

Although studies comparing soil evaporation, or K_e values, between two or more models/approaches in field and horticultural crops are scarce in the literature, some references were identified comparing crop evapotranspiration using energy balance models, both between them as with regard field measurements. For instance, Singh and Senay (2015) compared different energy balance models, reporting that the spatial and temporal variation of crop ET was reasonably well captured with an $R^2 > 0.81$ and errors around

0.9 mm day^{-1}. Similar coefficient of determination and estimated errors of around 25% between modelled and observed monthly ET data for orchards were recently determined by Volk et al. (2024) using the OpenET System. Furthermore, García-Santos et al. (2022) identified in a review about the TSEB model that the uncertainties obtained between this model and field measurements ranged from 0.6 to 2.4 mm d^{-1}. Thus, these indicators are in agreement to those obtained for the K_e (Table 4).

As shown in both Table 4 and Fig. 4, the crop coefficients increase in line with canopy cover due to its direct relationship with the $K_{cb\ A\&P}$ representing plant transpiration. However, the evaporative component (K_e) is mainly determined by the frequency and depth of rainfall or irrigation events, and the energy available at soil surface for water evaporation. This is why average $K_{e\ SWC}$ values were much higher during the initial and late stages than the mid-season (Table 4), and similar $K_{c\ A\&P+SWC}$ values were thus obtained regardless of the irrigation system for initial and end-season stages (differences between 0.02 and 0.07; Table 4), excepting in the autumn season of 2022 when rainfall events were much lower than the other seasons. In contrast, $K_{c\ A\&P+SWC\ mid}$ was between 0.05 and 0.13 higher for DI than SDI, thus contributing to improving the water consumptive use (less soil water evaporation) given by the subsurface drip irrigation.

Finally, the standard $K_{c\ A\&P+SWC}$ values obtained in this research (Table 4) are consistent with the range K_c values from 0.4 to 1.1 reported by García-Tejero et al. (2015) for 4-year-old almond trees in a lysimeter study, or the ranges of K_c from 0.3 to 1.2 observed by Drechsler et al. (2022) before harvest for a 4 year-old almond orchard. The former authors obtained a relationship between $K_{c\ mid}$ and the age of the almond tree, and those values, ranging from 0.40 to 1.0 for 1-year-old to 4-year-old, are very close to the values obtained for the mid-season in the present research, using a similar plant density (384 vs. 333 plants per hectare) although a different irrigation system (microsprinkler vs. drip).

Conclusions

This novel research has contributed to the literature by characterizing K_{cb} evolution across four growing seasons for a young drip-irrigated (surface and subsurface) almond orchard using the A&P approach, and evaluating its performance with regard to a simplified energy balance model (STSEB) upon weather data being corrected with respect to those conditions of a reference site. The following conclusions were obtained:

- The ET_o after correction of weather data by aridity conditions was reduced around 6% for the four studied seasons.
- The irrigation system did not generate differences in tree growth (in terms of $f_{c\ eff}$ and h) over the different years studied, with a single standard $K_{cb\ A\&P}$ for every growth stage and age tree being proposed, ranging between 0.15 at the initial stage of the second crop-greening to 0.97 in mid-season of the fifth crop-greening. Thus, over this study period, almond orchard architecture changed from a very low to a high degree of ground cover, identifying the inter- and intra-annual almond tree water requirements.
- Soil evaporation estimates were significantly different between the two irrigation systems, leading to the differences in K_e being around 16% higher for DI than SDI.
- As for K_{cb}, the K_c values increased as $f_{c\ eff}$ did, estimating from 0.30 in 2019 up to 1.01 computed under standard conditions, obtaining similar K_c values for the three K_c stages (i.e. $K_{c\ ini}$, $K_{c\ mid}$ and $K_{c\ end}$) because of the high K_e values obtained during the initial and late stages over the four growing seasons.
- In general terms, K_{cb} and K_e obtained using the A&P approach and the soil water balance (SWB) method, respectively, showed a good performance with respect to the STSEB estimates, reporting low errors of estimations and high goodness of fit.
- The A&P approach is especially interesting for estimating K_{cb} values in almond fruit trees, being useful for refining K_{cb} for conditions of plant spacing, size and density differing from standard values, where the M_L and F_r tabulated by López-Urrea et al. (2024) generated suitable results.

Acknowledgements This work was funded by the Education, Culture and Sports Council (JCCM, Spain) (project SBPLY/21/180501/000070) and the Agencia Estatal de Investigación (project TED2021–130405B-I00), together with FEDER and Next Generation EU/PRTR co-financing. F. Montoya thanks the JCCM (Spain) for the support to develop the SIMA project (SBPLY/21/180501/000152).

Author contribution Conceptualization, R.L.-U., J.G.-P. and J.M.S.; Methodology, R.L.-U., F.M. and J.M.S.; Software, F.M. and J.M.S.; Validation, F.M. and R.L.-U.; Formal analysis, F.M., J.M.S. and R.L.-U.; Investigation, R.L.-U., J.G.-P., F.M. and J.M.S.; Resources, R.L.-U., J.G.-P. and J.M.S.; Data curation, F.M.; Writing—original draft preparation, F.M.; Writing—review and editing, R.L.-U., J.G.-P. and J.M.S.; Visualization, R.L.-U.; Supervision, R.L.-U. and J.M.S.; Project administration, R.L.-U., J.G.-P. and J.M.S.; Funding acquisition, R.L.-U., J.G.-P. and J.M.S. All authors have read and agreed to the published version of the manuscript.

Data availability No datasets were generated or analysed during the current study.

Declarations

Conflict of interest The authors declare no competing interests.

References

Allen RG (1996) Assessing integrity of weather data for reference evapotranspiration estimation. J Irrig Drain Eng 122:97–106. https://doi.org/10.1061/(ASCE)0733-9437(1996)122:2(97)

Allen RG, Pereira LS (2009) Estimating crop coefficients from fraction of ground cover and height. Irrig Sci 28:17–34. https://doi.org/10.1007/s00271-009-0182-z

Allen RG, Pereira LS, Smith M et al (1998) Crop Evapotranspiration. guidelines for computing crop water requirements. Springer, Italy

Allen RG, Pereira LS, Smith M et al (2005) FAO-56 dual crop coefficient method for estimating evaporation from soil and application extensions. J Irrig Drain Eng 131:2–13. https://doi.org/10.1061/(ASCE)0733-9437(2005)131:1(2)

Allen RG, Tasumi M, Trezza R (2007) Satellite-based energy balance for mapping evapotranspiration with internalized calibration (METRIC)—model. J Irrig Drain Eng 133:380–394. https://doi.org/10.1061/(ASCE)0733-9437(2007)133:4(380)

Allen RG, Pereira LS, Howell TA, Jensen ME (2011a) Evapotranspiration information reporting: I. factors governing measurement accuracy. Agric Water Manag 98:899–920. https://doi.org/10.1016/j.agwat.2010.12.015

Allen RG, Pereira LS, Howell TA, Jensen ME (2011b) Evapotranspiration information reporting: II. Recommended Documentation Agric Water Manag 98:921–929. https://doi.org/10.1016/j.agwat.2010.12.016

Auzmendi I, Mata M, Lopez G et al (2011) Intercepted radiation by apple canopy can be used as a basis for irrigation scheduling. Agric Water Manag 98:886–892. https://doi.org/10.1016/j.agwat.2011.01.001

Bellvert J, Adeline K, Baram S et al (2018) Monitoring crop evapotranspiration and crop coefficients over an almond and pistachio orchard throughout remote sensing. Remote Sens 10:2001. https://doi.org/10.3390/rs10122001

Cancela JJ, Fandiño M, Rey BJ, Martínez EM (2015) Automatic irrigation system based on dual crop coefficient, soil and plant water status for Vitis vinifera (cv Godello and cv Mencía). Agric Water Manag 151:52–63. https://doi.org/10.1016/j.agwat.2014.10.020

De La Antonia GI (2023) Assessment of the correction of the reference evapotranspiration at nonirrigated weather stations affected by aridity and delimitation of the meteorological conditions that limit its implementation. Environ Process 10:40. https://doi.org/10.1007/s40710-023-00653-8

Domínguez A, Jiménez M, Tarjuelo JM et al (2012a) Simulation of onion crop behavior under optimized regulated deficit irrigation using MOPECO model in a semi-arid environment. Agric Water Manag 113:64–75. https://doi.org/10.1016/j.agwat.2012.06.019

Domínguez A, Martínez RS, De Juan JA et al (2012b) Simulation of maize crop behavior under deficit irrigation using MOPECO model in a semi-arid environment. Agric Water Manag 107:42–53. https://doi.org/10.1016/j.agwat.2012.01.006

Drechsler K, Fulton A, Kisekka I (2022) Crop coefficients and water use of young almond orchards. Irrig Sci 40:379–395. https://doi.org/10.1007/s00271-022-00786-y

Espadafor M, Orgaz F, Testi L et al (2015) Transpiration of young almond trees in relation to intercepted radiation. Irrig Sci 33:265–275. https://doi.org/10.1007/s00271-015-0464-6

FAOSTAT (2022) Food and Agriculture Organization of the United Nations. Stadistic Division. http://www.fao.org/faostat/en/#home

Fereres E, Martinich DA, Aldrich TM et al (1982) Drip irrigation saves money in young almond orchards. Calif Agric 36:12–13

Fereres E, Goldhamer DA, Sadras VO (2012) Yield Response to Water of Fruit Trees andVines: Guidelines. In Crop Yield Response to Water, FAO Irrigation and Drainage Paper, FAO: Rome, Italy, 505.ISBN 978-92-5-107274-5.

Fulton A, Grant J, Buchner R, Connell J (2014) Using the Pressure Chamber for Irrigation Management in Walnut Almond and Prune. University of California, Agriculture and Natural Resources

García-Santos V, Sánchez J, Cuxart J (2022) Evapotranspiration acquired with remote sensing thermal-based algorithms: a state-of-the-art review. Remote Sens 14:3440. https://doi.org/10.3390/rs14143440

García-Tejero IF, Hernández A, Rodríguez VM et al (2015) Estimating almond crop coefficients and physiological response to water stress in semiarid environments (SW Spain). J Agric Sci Technol 117:1255–1266

Girona J, Del Campo J, Mata M et al (2011) A comparative study of apple and pear tree water consumption measured with two weighing lysimeters. Irrig Sci 29:55–63. https://doi.org/10.1007/s00271-010-0217-5

Goldhamer DA, Fereres E (2017) Establishing an almond water production function for California using long-term yield response to variable irrigation. Irrig Sci 35:169–179. https://doi.org/10.1007/s00271-016-0528-2

IPCC (2022) Climate Change 2022. Impacts, Adaptation and Vulnerability. Working Group II contribution to the Sixth Assessment Report of the Intergovernmental Panel on Climate Change

Linnet K (1990) Estimation of the linear relationship between the measurements of two methods with proportional errors. Stat Med 9:1463–1473. https://doi.org/10.1002/sim.4780091210

López-López M, Espadafor M, Testi L et al (2018) Water requirements of mature almond trees in response to atmospheric demand. Irrig Sci 36:271–280. https://doi.org/10.1007/s00271-018-0582-z

López-Urrea R, De Santa M, Olalla F, Fabeiro C, Moratalla A (2006) Testing evapotranspiration equations using lysimeter observations in a semiarid climate. Agric Water Manag 85:15–26. https://doi.org/10.1016/j.agwat.2006.03.014

López-Urrea R, Oliveira C, Montoya F et al (2024) Single and basal crop coefficients for temperate climate fruit trees, vines and shrubs with consideration of fraction of ground cover, height, and training system. Irrig Sci Rev. 198:1–39. https://doi.org/10.1007/s00271-024-00964-0

Lorite IJ, Cabezas-Luque JM, Arquero O et al (2020) The role of phenology in the climate change impacts and adaptation strategies for tree crops: a case study on almond orchards in Southern Europe. Agric for Meteorol 294:108142. https://doi.org/10.1016/j.agrformet.2020.108142

MAPA (2023) Anuario de Estadística 2023. In: Minist. Agric. Pesca Aliment. https://www.mapa.gob.es/es/estadistica/temas/publicaciones/anuario-de-estadistica/default.aspx. Accessed 7 Jul 2024

Mcmaster G, Wilhelm W (1997) Growing degree-days: one equation, two interpretations. Agric for Meteorol 87:291–300

Mirás-Avalos JM, Gonzalez-Dugo V, García-Tejero IF, López-Urrea R, Intrigliolo DS, Egea G (2023) Quantitative analysis of almond yield response to irrigationregimes in Mediterranean Spain. Agric. Water Manag. 279: 108208. https://doi.org/10.1016/j.agwat.2023.108208

Montoya F, Sánchez JM, González-Piqueras J, López-Urrea R (2022) Is the subsurface drip the most sustainable irrigation system for almond orchards in water-scarce areas? Agronomy 12:1778. https://doi.org/10.3390/agronomy12081778

Norman JM, Kustas W, Humes K (1995) A two-source approach for stimating soil and vegetation energy fluxes from observations of directional radiometric surface temperature. Agric for Meteorol 77:263–293

Oyarzun RA, Stöckle CO, Whiting MD (2007) A simple approach to modeling radiation interception by fruit-tree orchards. Agric for

Meteorol 142:12–24. https://doi.org/10.1016/j.agrformet.2006.10.004
Paço TA, Ferreira MI, Rosa RD et al (2012) The dual crop coefficient approach using a density factor to simulate the evapotranspiration of a peach orchard: SIMDualKc model versus eddy covariance measurements. Irrig Sci 30:115–126. https://doi.org/10.1007/s00271-011-0267-3
Paço TA, Pôças I, Cunha M et al (2014) Evapotranspiration and crop coefficients for a super intensive olive orchard. an application of SIMDualKc and METRIC models using ground and satellite observations. J Hydrol 519:2067–2080. https://doi.org/10.1016/j.jhydrol.2014.09.075
Paço T, Paredes P, Pereira L et al (2019) Crop coefficients and transpiration of a super intensive arbequina olive orchard using the dual Kc approach and the Kcb computation with the fraction of ground cover and height. Water 11:383. https://doi.org/10.3390/w11020383
Paredes P, Martínez-Romero A, Petry M, et al (2024a) FAO56 crop growth stages estimation: setting base and upper temperature thresholds and cumulative growing degree days. Irrig Sci (Under review):
Paredes P, Petry MT, Oliveira CM et al (2024b) Single and basal crop coefficients for estimation of water requirements of subtropical and tropical orchards and plantations with consideration of fraction of ground cover, height, and training system. Irrig Sci. https://doi.org/10.1007/s00271-024-00925-7
Patrignani A, Ochsner TE (2015) Canopeo: a powerful new tool for measuring fractional green canopy cover. Agron J 107:2312–2320. https://doi.org/10.2134/agronj15.0150
Pereira LS, Allen RG, Smith M, Raes D (2015) Crop evapotranspiration estimation with FAO56: past and future. Agric Water Manag 147:4–20. https://doi.org/10.1016/j.agwat.2014.07.031
Pereira LS, Paredes P, Jovanovic N (2020a) Soil water balance models for determining crop water and irrigation requirements and irrigation scheduling focusing on the FAO56 method and the dual Kc approach. Agric Water Manag 241:106357–106357. https://doi.org/10.1016/j.agwat.2020.106357
Pereira LS, Paredes P, Melton F et al (2020b) Prediction of crop coefficients from fraction of ground cover and height. background and validation using ground and remote sensing data. Agric Water Manag 241:106197–106197. https://doi.org/10.1016/j.agwat.2020.106197
Pereira LS, Paredes P, Hunsaker DJ et al (2021a) Updates and advances to the FAO56 crop water requirements method. Agric Water Manag 248:106697. https://doi.org/10.1016/j.agwat.2020.106697
Pereira LS, Paredes P, López-Urrea R et al (2021b) Standard single and basal crop coefficients for vegetable crops, an update of FAO56 crop water requirements approach. Agric Water Manag 243:106196. https://doi.org/10.1016/j.agwat.2020.106196
Pereira LS, Paredes P, Melton F et al (2021c) Prediction of crop coefficients from fraction of ground cover and height: practical application to vegetable, field and fruit crops with focus on parameterization. Agric Water Manag 252:106663. https://doi.org/10.1016/j.agwat.2020.106663
Pereira LS, Paredes P, Oliveira CM et al (2023) Single and basal crop coefficients for estimation of water use of tree and vine woody crops with consideration of fraction of ground cover, height, and training system for Mediterranean and warm temperate fruit and leaf crops. Irrig Sci. https://doi.org/10.1007/s00271-023-00901-7
Pereira LS, Allen RG, Paredes P et al (2024) Crop evapotranspiration guidelines for computing crop water requirements, in press. Springer, Italy
Quintanilla-Albornoz M, Miarnau X, Pelechá A et al (2023) Evaluation of transpiration in different almond production systems with two-source energy balance models from UAV thermal and multispectral imagery. Irrig Sci. https://doi.org/10.1007/s00271-023-00888-1
R Core Team (2021) R: A language and environment for statistical computing
Raes D, Steduto P, Hsiao C, Fereres E (2023) Calculation procedures AquaCrop v. 7.1. Reference manual Chapter 3. Food and Agriculture Organization of the United Nations, Italy, pp 1–178
Rallo G, Paço TA, Paredes P et al (2021) Updated single and dual crop coefficients for tree and vine fruit crops. Agric Water Manag 250:106645. https://doi.org/10.1016/j.agwat.2020.106645
Ramos TB, Darouich H, Oliveira AR et al (2023) Water use and soil water balance of Mediterranean tree crops assessed with the SIMDualKc model in orchards of southern Portugal. Agric Water Manag 279:108209. https://doi.org/10.1016/j.agwat.2023.108209
Rosa RD, Paredes P, Rodrigues GC et al (2012a) Implementing the dual crop coefficient approach in interactive software: 2. Model Testing Agric Water Manag 103:62–77. https://doi.org/10.1016/j.agwat.2011.10.018
Rosa RD, Paredes P, Rodrigues GC et al (2012b) Implementing the dual crop coefficient approach in interactive software. 1. Background and computational strategy. Agric Water Manag 103:8–24. https://doi.org/10.1016/j.agwat.2011.10.013
Sánchez JM, Kustas WP, Caselles V, Anderson MC (2008) Modelling surface energy fluxes over maize using a two-source patch model and radiometric soil and canopy temperature observations. Remote Sens Environ 112:1130–1143. https://doi.org/10.1016/j.rse.2007.07.018
Sánchez JM, Simón L, González-Piqueras J et al (2021) Monitoring crop evapotranspiration and transpiration/evaporation partitioning in a drip-irrigated young almond orchard applying a two-source surface energy balance model. Water 13:2073. https://doi.org/10.3390/w13152073
SIAR (2022) Sistema de Información Climática para el Regadío. In: Minist. Agric. Pesca Aliment. https://eportal.mapa.gob.es/websiar/SeleccionParametrosMap.aspx?dst=1. Accessed 16 Mar 2022
Singh R, Senay G (2015) Comparison of four different energy balance models for estimating evapotranspiration in the midwestern United States. Water 8:9. https://doi.org/10.3390/w8010009
Stevens RM, Ewenz CM, Grigson G, Conner SM (2012) Water use by an irrigated almond orchard. Irrig Sci 30:189–200. https://doi.org/10.1007/s00271-011-0270-8
Thomas D (2018) Phenology standard for almonds shouth australian resarch and development institute PIRSA. Adelaide, Australia
Trigo IF, de Bruin H, Beyrich F et al (2018) Validation of reference evapotranspiration from meteosat second generation (MSG) observations. Agric for Meteorol 259:271–285. https://doi.org/10.1016/j.agrformet.2018.05.008
USDA-NRCS (2014) Keys to Soil Taxonomy. Unated States Department of Agriculture, 12th edn.
Volk JM, Huntington JL, Melton FS et al (2024) Assessing the accuracy of OpenET satellite-based evapotranspiration data to support water resource and land management applications. Nat Water 2:193–205. https://doi.org/10.1038/s44221-023-00181-7
Willmott CJ (1982) Some comments on the evaluation of model performance. Bull - Am Meteorol Soc 63:1309–1313. https://doi.org/10.1175/1520-0477(1982)063%3c1309:SCOTEO%3e2.0.CO;2